Rapid Mangrove Forest Loss and Nipa Palm (Nypa fruticans) Expansion in the Niger Delta, 2007-2017

remote sensing

MDPI

Article

Rapid Mangrove Forest Loss and Nipa Palm (*Nypa fruticans*) Expansion in the Niger Delta, 2007–2017

Chukwuebuka Nwobi [1,2,*], Mathew Williams [1,2] and Edward T. A. Mitchard [1]

[1] School of GeoSciences, University of Edinburgh, Edinburgh EH9 3FF, UK; mat.williams@ed.ac.uk (M.W.); edward.mitchard@ed.ac.uk (E.T.A.M.)

[2] National Centre for Earth Observation, University of Edinburgh, Edinburgh EH9 3FF, UK

* Correspondence: ebuka.nwobi@ed.ac.uk; Tel.: +44-1316-517-112

Received: 29 May 2020; Accepted: 17 July 2020; Published: 21 July 2020

Abstract: Mangrove forests in the Niger Delta are very valuable, providing ecosystem services, such'as carbon storage, fish nurseries, coastal protection, and aesthetic values. However, they are under threat from urbanization, logging, oil pollution, and the proliferation of the invasive Nipa Palm (*Nypa fruticans*). However, there are no reliable data on the current extent of mangrove forest in the Niger Delta, its rate of loss, or the rate of colonization by the invasive Nipa Palm. Here, we estimate the area of Nipa Palm and mangrove forests in the Niger Delta in 2007 and 2017, using 567 ground control points, Advanced Land Observatory Satellite Phased Array L-band SAR (ALOS PALSAR), Landsat and the Shuttle Radar Topography Mission Digital Elevation Model 2000 (SRTM DEM). We performed the classification using Maximum Likelihood (ML) and Support Vector Machine (SVM) methods. The classification results showed SVM (overall accuracy 93%) performed better than ML (77%). Producers (PA) and User's accuracy (UA) for the best SVM classification were above 80% for most classes; however, these were considerably lower for Nipa Palm (PA—32%, UA—30%). We estimated a 2017 mangrove area of 801,774 ± 34,787 ha (±95% Confidence Interval) ha and Nipa Palm extent of 11,447 ± 7343 ha. Our maps show a greater landward extent than other reported products. The results indicate a 12% (7–17%) decrease in mangrove area and 694 (0–1304)% increase in Nipa Palm. Mapping efforts should continue for policy targeting and monitoring. The mangroves of the Niger Delta are clearly in grave danger from both rapid clearance and encroachment by the invasive Nipa Palm. This is of great concern given the dense carbon stocks and the value of these mangroves to local communities for generating fish stocks and protection from extreme events.

Keywords: mangrove; Nipa Palm; land cover classification; change detection; invasive species; deforestation

1. Introduction

Mangrove ecosystems are intertidal regions at the land-sea, fresh-salt water interface; hence, they have characteristics of both zones. Mangrove systems also have peculiar properties, such as anaerobic conditions, salinity fluctuation, and tidal influence [1]. Mangrove ecosystems in the world are of great ecological, economic, and social importance [2–4] because they are important carbon stores, supportive of the lives of coastal human populations who depend on fisheries. Mangrove forests also serve as a direct means of coastal protection from storm surges, tidal waves, and, over longer time scales, provide resilience to climate-change driven sea level rise. The ecosystem services provided by mangrove forests are under threat from natural and anthropogenic factors. The superimposition of mangroves with the high population density of coastal communities has resulted in rapid and

increasing deforestation [5]. Deforestation can be because of mangrove clearance for fuelwood and fisheries, agriculture, industrial pollution, and urbanization in coastal regions. In south-east Asia, aquaculture, and agriculture are the major drivers of deforestation in mangrove forests [6], while in oil producing countries, oil pollution, which results in fire largely contributes to mangrove deforestation in these regions [7]. Mapping mangrove forest cover across space and time can help provide information on the progress of restoration programs and detect areas of high mangrove deterioration, enabling conservation targeting, and policy implementation [5].

Mangrove mapping has improved as suitable satellite data and analysis tools have proliferated; however, the reliability of these maps is dependent on validation. Fieldwork in mangroves is always difficult, as their tidal nature and obstructive root systems make it difficult to access areas, measure trees, or set up plots [8]. The first attempt to estimate global mangrove area was done by Spalding et al. (1997), estimating about 181,000 km^2 in 1997 [9]. They estimated mangrove area using a combination of regional maps and ground-truth data. Giri et al., (2011) estimated the global mangrove area in 2000 as 137,760 km^2 using about 1000 Landsat scenes, ground truth data, regional maps and a combined supervised (driven by ground data) and unsupervised (driven by clusters in the remote sensing layers) classification techniques [10]. The Global Mangrove Watch has reported a new 2010 baseline for global mangrove area of 137,760 km^2 using a combination of Advanced Land Observatory Satellite Phased Array L-band Synthetic Aperture Radar (ALOS PALSAR), Landsat data and Extremely Randomized Tree classifiers [11]. They reported an accuracy of 94% against some ground control sites globally, although this could vary on regional basis as there was no site in West Africa.

The differences in areas reported in the previous paragraph could partly be due to errors, but is also likely due to changes in the area of mangroves over the differing time period of the map. Global mangrove area change has been reported a global loss of 8 437 km^2 between 1996 and 2016 [12]. Thomas et al., (2017) reported that 71% of radar tiles representing global mangrove forests in their analysis were intact while 37.8% represented total anthropogenic activity between 1996 and 2010. Mangrove loss regionally was greatest in Southeast Asia and global driver for anthropogenic mangrove loss was conversion to agriculture [13]. They reported that in Africa, while 12,641 km^2 of the mangrove area was intact, 6186 km^2 represented anthropogenic loss. However, others have reported regional mangrove area gain [14]. Thomas et al. (2018) reported that the Niger Delta had a mangrove area net gain of 8490 ha between 1996 and 2010. Another report shows that global mangrove area lost 3,563,000 ha between 1980 and 2005 with 14% of this was accounted for by Africa [15]. Food and Agriculture and Organization (FAO), (2007) reported that Nigeria lost 2000 ha of mangrove area between the same period (1980–2005), which accounted for only 0.4% of mangrove loss in Africa [15]. The Global Mangrove Watch also reported a change of 6081 km^2 of global mangrove area between 1996 and 2016 with Nigeria losing between 1–2% of the mangrove within this period [11]. The various reports of global and regional mangrove change shows the need for more local studies in order to extract accurate information. The change in global area of mangroves should be analyzed regionally in order to target conservation efforts based on accurate data.

In this study, we focus on the extensive, understudied and rapidly changing mangroves of the Niger Delta. The Niger Delta is located on the central coast of Nigeria and is influenced by the Gulf of Guinea. It has a human population of 28 million (2005) and a land surface area of 11 million ha [16]. The Delta is a hub of the Nigerian economy because the oil industry of the country is largely based in the Delta, and directly contributes about 10% to Nigeria's Gross Domestic Product (GDP) [16,17]. The region also supplies fish and timber products to the rest of the country [18,19]. In Nigeria, mangroves provide erosion control, climate change regulation, wood for fuel and construction, sacred sites and fisheries [7]. However, oil pollution, urbanization, and over-exploitation for fuelwood are major causes of mangrove degradation and loss [20]. Fuelwood exploitation by coastal communities of mangrove stands results in a change of the forest stand structure or canopy structure. These changes can result in loss of large tree stems and forest gap formation fostering invasion by non-native species [21].

A further identified source of the degradation of Nigeria's mangroves is the alien invasive mangrove palm, *Nypa fruticans*, a mangrove palm commonly known as the Nipa Palm, native to the Indian Ocean coast. Non-native species are known to proliferate in damaged ecosystems, and can lead to a change in community structure and biodiversity by altering the function of the ecosystem [22]. Nipa Palm was introduced in the Calabar estuary of Nigeria, to the east of the Niger Delta, in 1906 to serve as a plantation for beautification and beach erosion control [23]. However, Nipa Palm spreads rapidly through its water-borne seeds, and has proliferated rapidly along Nigeria's coast. This spread has been assessed by poor management of plantations, as well as actions that degrade mangroves, letting the Nipa Palm in, including unsustainable logging activities, dredging, and oil pollution [24,25]. Nipa Palm spread is further compounded by the lack of use of this palm as a resource, as it is in Asia and Oceania where its fruit is eaten and used to produce juice, and palm fronds used for roof construction [26]. Therefore, anecdotal studies suggest Nipa Palm is gradually replacing mangrove forests in the Niger Delta, especially in areas of high exploitation [27]. Various attempts have been made to use Nipa Palm's potential products, which include its sap (which is sugar rich), its tannins, its potential for bioenergy products, and its palm leaves as a building material [24,28,29]. However, the location of the Nipa Palm along the tidal channels places it at an unfavorable location for transportation of the resource generated. The United Nations published a report in 2007 on possible control measures of Nipa Palm infestation in Nigeria [30]. There has also been a proposal for the utilization of Nipa Palm as a renewable source of energy [24]. Cultural management of Nipa Palm spread is undertaken by the removal of Nipa Palm seedlings in some parts of the Niger Delta, but there are no reports of a large-scale management plan of Nipa Palm invasion in the Niger Delta. Monitoring the extent of native species and the spread of invasive species can provide the key to controlling alien species and managing the conservation of the native species [31]. Therefore, monitoring vegetation over space and time is essential for successful management of Nipa Palm, as well as for other threats to mangroves forests in the Niger Delta.

Satellite remote sensing offers an appropriate method for mapping land cover (LC) and LC change. Remote sensing data splits broadly into two types: passive or active [32]. Passive sensors use reflected solar radiation to monitor the observed region, while active sensors emit signals that interact with surface or sub-surface features [33]. Passive sensors such as optical data are sensitive to the greenness of an ecosystem, while active sensors have the penetrative power to retrieve forest structure including the woody biomass. Passive sensors can be excellent at monitoring productivity and the degree of canopy cover, given their sensitivity to the contrast between green vegetation and non-vegetated surfaces. However, optical data are often masked by cloud cover, which is always a problem in coastal tropical regions [5]. In contrast, active sensors such as Synthetic Aperture Radar (SAR) record the surface structures [34–36]. Medium and long-wavelength (C-band or longer) Synthetic Aperture Radar (SAR) data do not suffer from cloud cover, and obtain complementary information to optical data about forested systems. In particular, this is true of longer-wavelength SARs (L-band or longer), as their data penetrate the forest canopy and given information on forest structure. However, these SAR data have been more rarely used for classification of mangrove systems because of poorer data availability, more complex processing, lower resolution and more noisy data, and higher costs, than optical data (which are often free). However, the release by Japanese Aerospace Exploration Agency (JAXA) of the Kyoto and Carbon mosaics of Advanced Land Observatory Satellite Phased Array L-band Synthetic Aperture Radar (ALOS PALSAR) data has made long-wavelength SAR data far easier to use [37].

Although these two sensor types can be used separately, more recent studies have fused the two to achieve higher accuracy in analysis due to their combined individual strengths [11,35,38,39]. The Landsat and Sentinel-2 and sensors have been acquiring optical data at moderate (10–30 m) resolution since the 1970s and 2015, respectively, and are openly available. Although most scenes captured by these satellites over mangrove regions are cloudy, optical data can still be used through the stitching together of cloud-free portions of many images to make cloud-free composites, and in combination with SAR data.

There are various factors involved in choosing the classification algorithm to use for optimal LC discrimination from remote sensing data. LC classification can be done using unsupervised or supervised methods. Unsupervised classification predicts different classes based on statistics from the spectral characteristic of the satellite products; while supervised methods predict LC types using ground control points as training data [40]. A simple and common supervised classification method is the Maximum Likelihood (ML) classifier; a parametric method that assumes a normal distribution of the multispectral data, and that is highly computationally efficient [41,42]. The Support Vector Machine (SVM) classifier, contrary to ML, is non-parametric, making no assumption about the data distribution. SVM identifies the optimum boundary between training classes utilizing the edge of the class distribution [43,44]. This optimum boundary can also be referred to as the Optimum Separation Hyperplane (OSH), while the training samples at the class distribution edge can be referred to as the support vectors [40,45]. The accuracy of SVM has been shown to be better than ML, Artificial Neural Networks (ANN), and decision trees, especially when training datasets are comparatively small [42,46,47]. However, the use of SVM and ML in detecting fringe invasive species is largely unstudied. Mapped results are validated for accuracy by comparing with other mapped products, using accuracy assessments or field verification [48].

The development of a spatiotemporal map of mangrove cover for Nigeria could be valuable as it would form a baseline for mangrove conservation and restoration. Mangrove extent in the Niger Delta has been estimated by James et al. (2007) and Fatoyinbo and Simard (2013), both using an unsupervised classification ISODATA method to estimate mangrove area from Landsat Enhanced Thematic Mapper Plus (ETM+) [49,50]. These studies show the ability of remote sensing options in estimating mangrove area without the need for training data. However, the use of ground truth data and fused radar/optical data has not been explored in the estimation and change detection of coastal vegetation in the Niger Delta.

Here therefore, we estimate mangrove forest and Nipa Palm cover in the Niger Delta between 2007 and 2017. We compare the accuracy of ML and SVM in estimating coastal vegetation, in order to provide a steer to other studies. Specifically, we aimed to:

1. Compare the two different types of land cover classification in estimating mangrove area;
2. Estimate the extent of mangrove and Nipa Palm and;
3. Detect and report the change of mangrove and Nipa Palm area between 2007 and 2017.

From our knowledge of the literature [42,44,45,51], we hypothesized that SVM will have a better accuracy than ML in predicting LC classes using fused data. We also predicted from our knowledge of the region that mangrove area will have reduced in the delta due to deforestation, and Nipa Palm extent increased, over the study period.

2. Materials and Methods

2.1. Study Area

The Niger Delta study region (Figure 1) spans from the Benin River estuary in the west to the Calabar river estuary in the east. Economic activity is primarily farming within these regions while fuelwood and fisheries account for minor sources of income [19]. Increased urbanization is occurring including road construction, port establishment and settlement building [27]. Mangroves species zonation is influenced by saline conditions [52–54]. However, Nipa Palm interrupts this zonation along mangrove fringe and inland sections where exploitation for timber or fuelwood has taken place [23].

2.2. Field Data and Sampling Strategy

We carried out three field surveys for eight months across the Niger Delta: September 2016–January 2017 and June–August 2017. We adopted a multiclass method consisting of 6 broad vegetation classes, chosen from our knowledge of the region during fieldwork and the literature (Figure 2, Table 1). These classes were chosen in order to focus on mangrove and Nipa Palm. The other classes gave a general overview of other land cover types in the region.

During the fieldwork, we collected 567 ground control points (GCPs) across the East–West Highway (which connects the entire coastal state); during surveys on a boat, and during sample collection (Figure 1). We used an opportunistic sample scheme to collect GCPs due to security issues ranging from kidnapping, oil bunkering and militancy [55]. We recorded the type of land cover class, GPS coordinates using a Garmin eTrex 20x device (≤10 m error); and at the end of each day, we used Google Earth Pro application to delineate the areal extent of each of land cover class. Areas of interest during GCP selection were islands off the Calabar estuary and along the Imo river estuary where a clear transition of Nipa Palm, to mangrove forests, then to agricultural lands or terra forma forests was observed. Another essential region were creeklets in Rivers State where settlements were surrounded by a transition of mangrove forests and rainforests. We selected points with distinct spectral characteristics in order to improve accuracy and validation of the classification output. Despite not having GCPs in 2007, we used Google Earth Pro application to locate the GCPs collected during the field campaigns and assess if they were a different or the same class in 2007 using the timeline tool. We removed GCPs where their locations were obscured by cloud in the image data. We used 417 stable GCPs in the supervised classification in 2007.

The GCPs over the entire region were uneven because of the proportional cover of the different classes over the Niger Delta region. Hence, we collected more training pixels for classes with more coverage to classify the land classes in relation to their proportion. We divided the GCPs between training and testing in a ratio of 70% for training the classification algorithm and 30% for testing map accuracy.

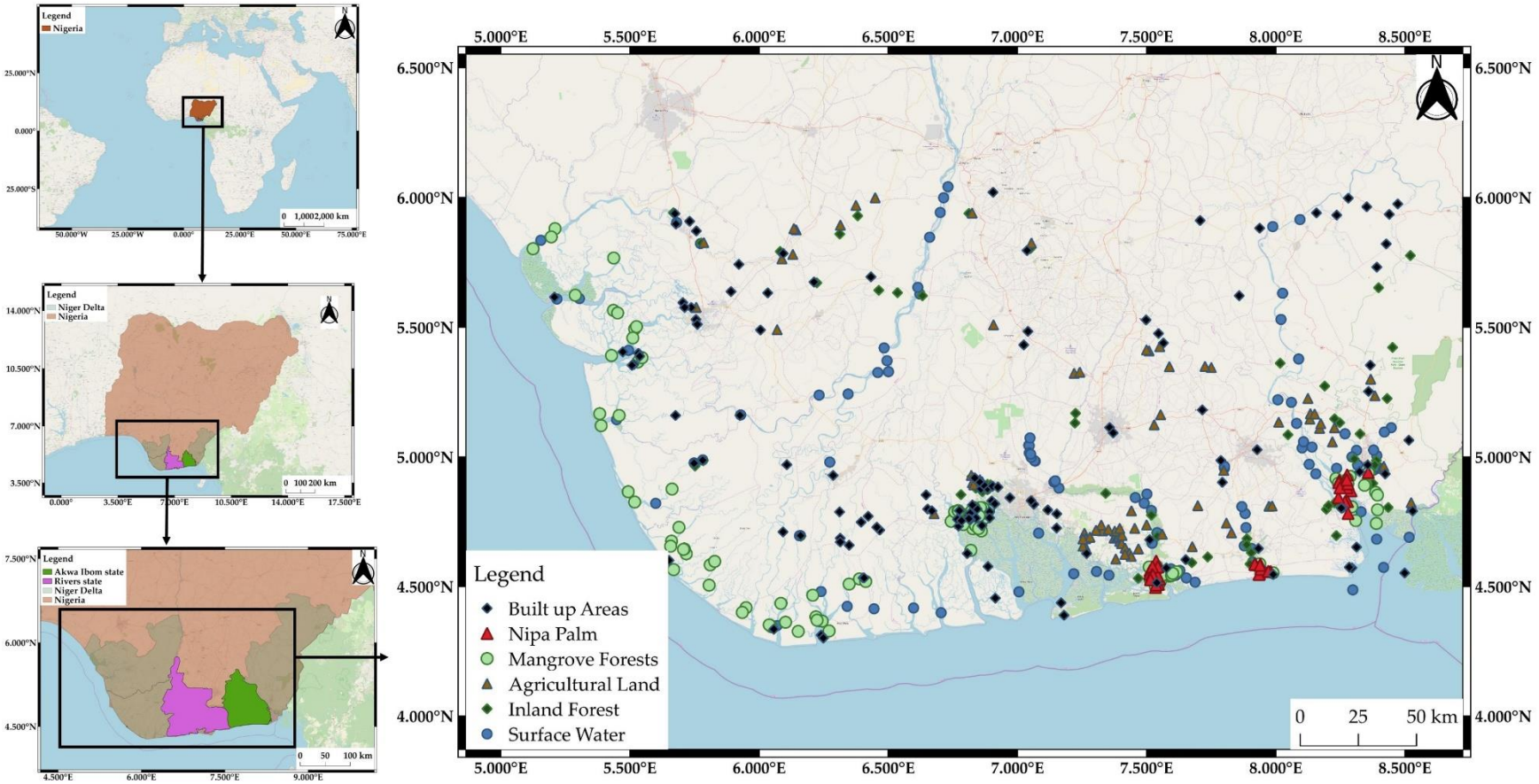

Figure 1. Location of Nigeria in West Africa, the Niger Delta in Southern Nigeria, study area, and ground control points (GCPs) established during the field survey.

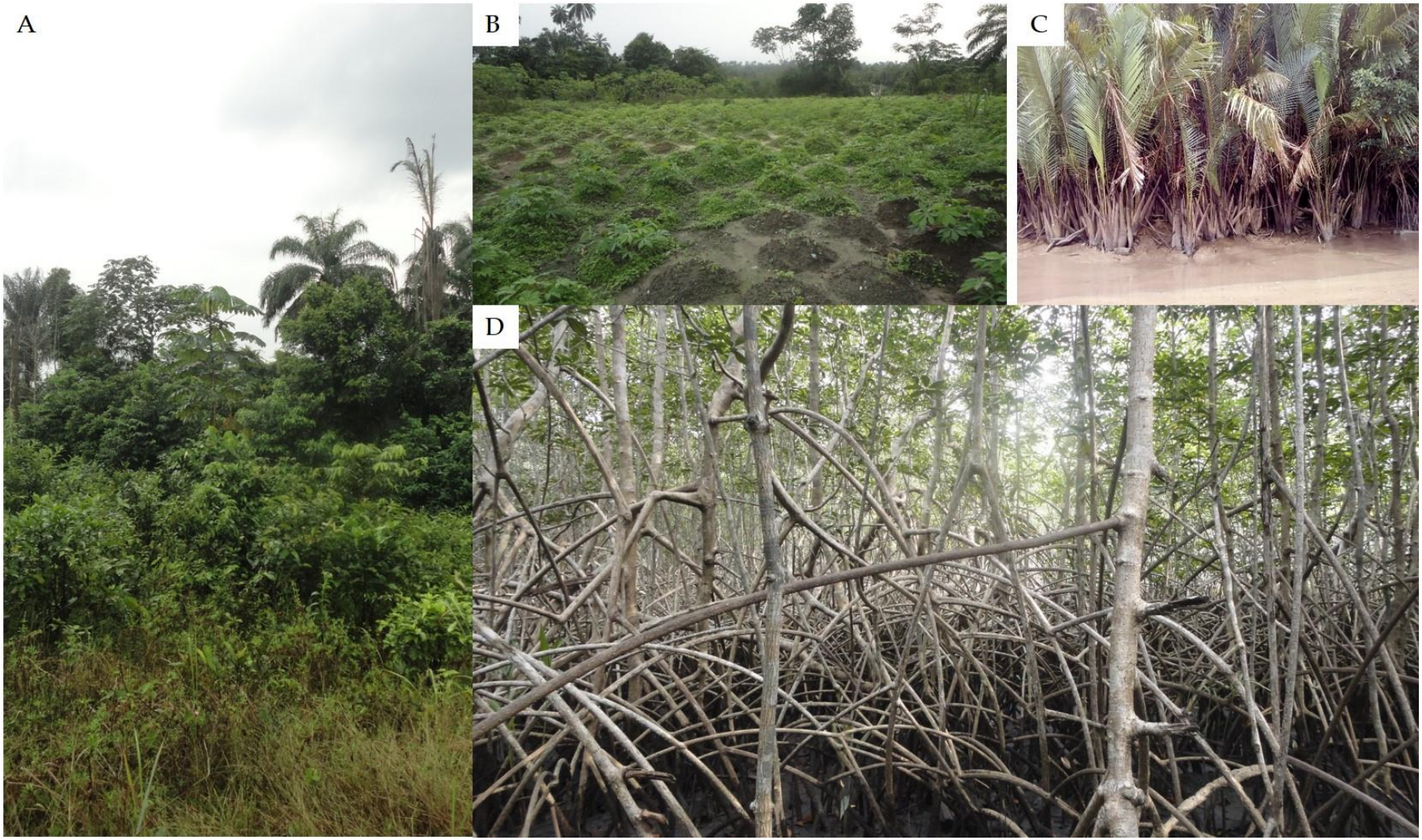

Figure 2. Land cover classes used in land cover classification. (**A**) Terra firma Forest; (**B**) agricultural land; (**C**) Nipa Palm; (**D**) mangrove forest.

Table 1. Number of pixels from Google Erath generated polygons of land cover classes for 2007 and 2017.

No	Class Name	Description [1]	Training Pixels (2017)	Testing Pixels (2017)	Training Pixels (2007)	Testing Pixels (2007)
1	Mangrove Forests	Mangrove forests located in intertidal regions strictly vegetated with red (*Rhizophora* spp.), black (*Avicennia germinans*) or white (*Laguncularia racemosa*) mangrove species.	25,522	3453	31,956	4842
2	Nipa palm	Nipa Palm stands within mangrove forests or along the fringes.	751	62	103	53
3	Terra firma forests	All other forested vegetation, palm plantations and evergreen forests	257,398	2338	252,798	4172
4	Surface water	All areas with open water including coastal waters.	249,912	2562	249,983	3216
5	Built up regions	Developed land with constructed structures including industries, residential area, roads	2931	1953	52,341	5876
6	Agricultural land	Cultivated land, pastures, other herbaceous vegetation, parks	2864	2864	68,329	5777

[1] based on field surveys.

2.3. Earth Observation (EO) Data

2.3.1. Digital Elevation Model (DEM)

The SRTM acquired data at both X and C-SAR bands designed for single-pass operation interferometry [56]. This data filled gaps and voids with elevation data primarily from the Terra Advanced Space borne Thermal Emission and Reflection Radiometer (ASTER) Global Digital Elevation Model Version 2.0 (GDEM 2) and secondarily from the U.S. Geological Survey (USGS) Global Multi-resolution Terrain Elevation Data (GMTED) 2010 [57]. We also used the SRTM DEM in order to aid the LC classification of the Niger Delta because we know that such sea-influenced vegetation will change with elevation above sea level [58]. Mangrove and Nipa Palm vegetation occur at the intertidal zones of the coast. Hence, this will significantly aid in differentiating coastal vegetation from other vegetation types. We downloaded the SRTM DEM 1 arc sec global version 3 data for twelve tiles covering the Niger Delta using Earth Explorer.

2.3.2. Synthetic Aperture Radar (SAR)

The Japanese Aerospace Exploration Agency (JAXA) has successfully launched EO missions in order to monitor disaster, cultivated land, increase data archives and tropical rainforests [59]. These missions include the Advanced Land Observing Satellite 1 and 2 (ALOS and ALOS-2). ALOS-2 was a sequel to ALOS "DIACHI", launched in May 2014 [60]. ALOS-1 and 2 both used the Phased Array type L-band Synthetic Aperture Radar (PALSAR). The L-band SAR scenes we used were acquired in Fine Beam Dual (FBD) polarization mode with off-nadir angle averaging 34.3° for ALOS PALSAR and multi-looked pixel size of 0.8 arc sec (~25 m).

Pre-processing SAR data is complicated—there are many steps involved in geo-rectifying and terrain correcting the raw satellite data. In order to increase the usability of the data, JAXA have produced pre-processed mosaics where they have performed these steps in advance using the JAXA Sigma-SAR processor [61]. Unlike raw data, these data are also available without charge for research use. We downloaded raw ALOS PALSAR and ALOS-2 PALSAR-2 25 m Mosaic files (HH and HV bands) from the JAXA, Earth Observation Research Centre (http://www.eorc.jaxa.jp/ALOS/en/index.htm) for the years 2007 and 2017. The data tiles were N07 E002, N07 E003, N07 E004, N07 E005, N07 E006, N07 E007, N07 E008, N06 E004, N06 E005, N06 E006, N06 E007, N06 E008, N05 E005, N05 E006, N05 E007, and N05 E008.

2.3.3. Landsat Data

Landsat ETM+ 7 Collection 1 Tier 1 Digital Number values from the study region was downloaded and pre-processed to remove cloud cover using the Google Earth Engine (GEE) [62].

2.4. Image Processing

All spatial analyses were undertaken within ENVI version 5.1 [63], QGIS [64], Google Earth Engine (GEE) [62], Google Earth Pro (GEP) [65] and ArcGIS [66]. Three datasets were used for LC classification: SRTM DEM, ALOS PALSAR and Landsat 7 ETM+ (Figure 3). We imported ground control points (GCPs) into GEP to generate polygons based on information from field surveys. QGIS and ArcGIS were used to convert the polygons to shape file format, re-project and dissolve to the land cover classes. GEE was used to pre-process and download Landsat data. ENVI was used to pre-process digital elevation model and radar data, carry out classification and post classification. Details of these processes are given in the sections below.

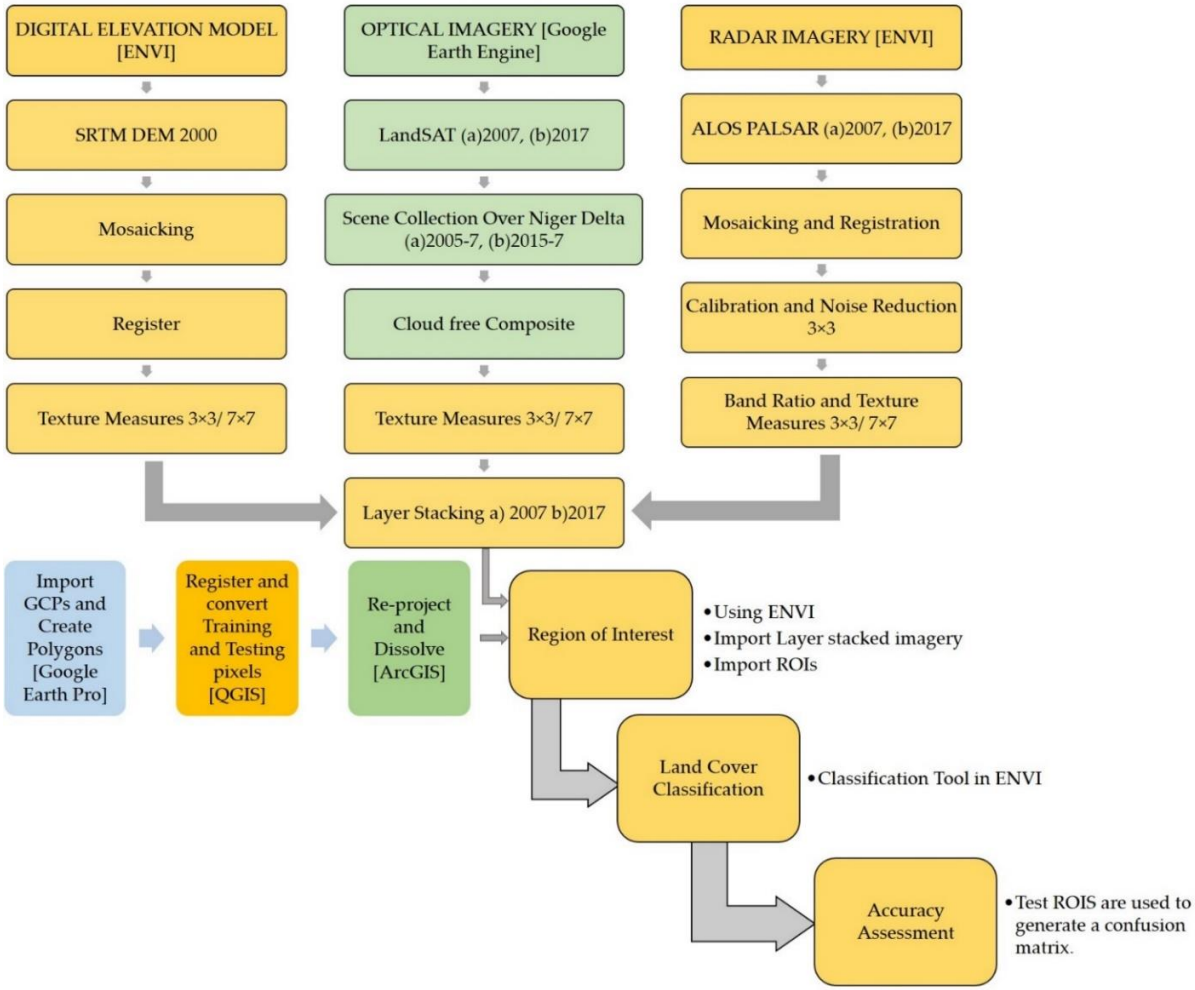

Figure 3. Image processing steps prior to land cover (LC) classification. Digital Elevation Model (DEM), Advanced Land Observing Satellite (ALOS) Phased Array L-band Synthetic Aperture Radar (PALSAR) and Landsat were pre-processed separately before they were stacked together with the Shuttle Radar Topography Mission (SRTM) DEM 30 m resolution. We grouped both Landsat and ALOS PALSAR data for the year 2007 and 2017. Each color code represents the different software used for analysis.

2.4.1. Synthetic Aperture Radar (SAR)

We mosaicked individual data tiles to form a single image file of the Nigerian coastline in both bands and geo-referenced with the projection Universal Transverse Mercator (UTM) Zone 31 North and World Geodetic System (WGS) 1984 datum. The image file of both bands was registered using 41 GCPs in Landsat bands of Hansen et al., (2013) and using a first order polynomial approach (RMS error = 0.27) which was sufficient for data analysis [67].

Calibration of ALOS PALSAR backscattering on the image through two stages. We first converted the digital number (DN) value on the original image to decibel (dB) (Equation (1)) based on the coefficients and equations from Shimada et al., (2009) [68]. We used single year tiles (2007 and 2017) for the LC classification.

Conversion of DN to

$$\sigma^0 \text{ (dB)} = 10 \times (\log_{10} (\text{DN}^2)) - 83, \quad (1)$$

Speckle associated with Synthetic Aperture Radar (SAR) data reduces the efficiency of class characterization by affecting the radiometric and textural qualities. However, filtering processes can reduce the impact of speckle. These filtering techniques can reduce or eliminate the information contained in the image, in particular resulting in a smoothing out of the (real) hard boundary between two land cover types [69,70]. Adaptive filters have been developed to attempt to reduce this problem: and thus, we used the Enhanced Lee Filter to reduce the speckle. Adaptive filtering makes a choice about how to average a pixel based on its neighborhood. The Enhanced Lee Filter determines the grey level for each pixel by computing the weighted sum of the center pixel value, the mean value, and the variance calculated in a square kernel surrounding the pixel. This filter is used primarily to suppress speckle by smoothening image data without removing edges or sharp features in the images while minimizing the loss of radiometric and textural information [71].

We carried out the filtering process in this study used a 7×7 window on both HH and HV bands to minimize the loss of information in the image, which gives the best results for classification based on published results [71,72]. After the conversion of digital value to the backscatter coefficient (σ^0) and speckle reduction performed, the ratio of HV to HH was calculated after transformation into the power domain (P) (Equation (2)). This ratio has been shown to contain further information useful for classification, by giving information on the comparative strength of different scattering mechanisms.

Conversion of σ^0 to

$$\text{power (P)} = 10^{(\sigma^0/10.0)}, \quad (2)$$

2.4.2. Landsat Data

A cloud-free composite was created using the ee.Algorithms.Landsat.simpleComposite() method, which allows the creation of a composite from and image collection (stacked images). This algorithm selects the median value for each band of each pixel. We ensured median composites were cloud free over the period by building up the collection using pixels with less than 5% cloud cover over the time-series. In order to assess two different years, we created a composite of Top of the Atmosphere (TOA) data from 2005 and 2007; and from 2015 and 2017. We also calculated the cloud score of the scenes in the Landsat collection used in the creation of a cloud free composite. The GEE code can be assessed here: https://github.com/ebukanwobi/Landsat-Scene-Code-Niger-Delta through a GIT repository.

2.4.3. Texture Measure

We performed first order occurrence statistics on the DEM, and all ALOS PALSAR and Landsat 7 ETM+ bands. We applied a 3 × 3 and 7 × 7 window size for all image texture analysis for comparison. The window size has the advantage of capturing the heterogeneity of pixel values over edges of different land cover classes, especially mangrove- Nipa Palm interface. However, texture measures with higher window sizes can reduce the quality of the image for analysis. We selected texture measures based on their established ability to characterize vegetation structure. We calculated three first order texture measures (data range, mean and variance) using the ALOS PALSAR and Landsat 7 bands. We chose these measures because they had the highest ROI separability between mangrove and Nipa palm.

2.4.4. Layer Stacking

We stacked all EO data for both years (2007 and 2017) using a 30 m scale (Table 2).

Table 2. Earth Observation (EO) data used for classification.

Data	Date	Bands	Texture Measures
SRTM DEM	2000	Elevation	-
ALOS PALSAR	2007, 2017	HH, HV, HV:HH	data range, mean and variance
Landsat 7	2005–2007, 2015–2017	1 (blue), 2 (green), 3 (red), 4 (Near Infrared), 5 (Short-wave Infrared 1) and 7 (Short-wave Infrared 2)	data range, mean

SRTM DEM: Shuttle Radar Topography Mission Digital Elevation Model, ALOS PALSAR: Advanced Land Observatory Satellite Phased Array L-band Synthetic Aperture Radar, HH: horizontal send, horizontal receive, HV: horizontal send, vertical receive.

2.5. Supervised Classification

We implemented ML and SVM to classify the layer stacked data for 2007 and 2017 into six classes. We masked any 'no data' pixels within bands for the ML to avoid errors during statistics computation. We also tested ML classification for various band combinations for comparison including:

- 3 SAR bands + SRTM DEM;
- 6 Landsat bands + SRTM DEM;
- a combination of both Landsat and SAR data + SRTM DEM;
- a combination of SRTM DEM, SAR, Landsat and texture measures using 3 × 3;
- a combination of SRTM DEM, SAR, Landsat and texture measures using 7 × 7.

The kernel function in SVM involves a choice of how to represent the data in higher dimensional space [73]. This dimensional space could be radial basis function, sigmoid and polynomial. The penalty parameter (C) is the degree of how much error given in the classification. A higher C will result in minimal error [74]. Gamma is a function of how the distance between training data affect the similarity of the training points. This only applies to non-linear kernel and we used the default value (inverse of the number of bands used in the classification- 31 bands). We tested two types of kernel type for SVM classification based on results of Yang, (2011) who tested various parameters of SVM in a LC classification [75].

- Linear Kernel type, Penalty Parameter (100).
- Linear Kernel type, Penalty Parameter (50).
- Radial Basis Function (RBF) Kernel Type, Gamma in Kernel Function (0.032), Penalty Parameter (100).
- Polynomial Kernel Type, Gamma in Kernel Function (0.032), Penalty Parameter (100).
- In order to carry out a change detection analysis, we classified the same set of data for both years, 2007 and 2017.

2.6. Accuracy Assessment

We assessed the performance of the classification results by carrying out post classification confusion matrices and overall accuracies using testing pixel (Table 1) independent of the training pixels. We used identical training and testing pixels for the different types of classifiers to minimize bias separately for both years. We placed particular interests in the following confusion matrix variables: Overall accuracy (a measure of how accurate the classified classes), Producer's accuracy (PA; the probability of how accurate each of the classes were classified), and User's accuracy (UA; the probability that a certain class prediction belongs to that class) [76].

We used prior knowledge of the study site from both fieldwork and communication with the locals, as well as Google earth timeline images. Areas of focus for the visual search included roads; urban areas embedded within larger forest, and forest-urban-mangrove boundary. We also reported the individual confusion matrices of the different land cover classes.

We used the PA and UA to calculate 95% confidence intervals (CI) for areas of each land cover classes. This method of 95% CI for areas was based on Olofsson et al., (2014) using stratified random sampling based on single year classification [77].

2.7. Change Detection

We performed change detection analysis of the resultant LC types using the change detection statistics tool in ENVI. This tool analyses the change from a base initial image for each class. It does this by evaluating the number and percentage of pixels change in classes between the initial and final images. The time intervals investigated in this study were 2007 (initial) to 2017 (final).

3. Results

3.1. Accuracy Assessment

Overall accuracies from the SVM classifications for 2017 (93%) was greater than the ML method (77%). Using ML method, classification based on Landsat bands (66.8%) performed better than SAR bands (44.4%) (Table 3). Accuracy improved using a combination of Landsat and SAR bands (67.4%). Inclusion of texture measures also improved LC classification with 3×3 window size (77%) performing slightly better than the 7×7 (76.9%). Using a combination of SRTM DEM, SAR, Landsat and texture measures using 3×3, the overall accuracy (92–93%) did not differ amongst the kernel types tested in the SVM method (Table 3). Surface water; urban regions and agricultural lands were easily detected with PA above 90% for all SVM classifiers (Tables 3, A1 and A2). The mangrove class had the lowest producer's accuracy (65%) in the ML, but fortunately had much better accuracies (>90%) when using the SVM methods (Table 3). We also discovered that while the highest producer's accuracy (100%) on the Nipa Palm invasive species was in the ML method, it also had a very low user's accuracy (5%) (Table 3), with further investigation showing this was due to overestimation (Figure 4). The accuracy of Nipa Palm classification was low using all other methods, with even the best SVM method (RBF) achieving a User's and Producer's Accuracy of 32% and 30% respectively. However, as these were relatively balanced, we hope that the area estimate of Nipa Palm from the classification remains reasonably accurate, and certainly these low accuracies will feed into the confidence interval estimates so useful ranges of area are still available from the analysis (See Table 6).

We decided that the best classification results were from the SVM method under the Radial Basis Function kernel type, which had the highest classification and user's accuracy for mangrove (89%, 93%) and Nipa Palm (32%, 30%). There was high confusion of Nipa Palm with both surface water and mangrove forests because of the class transition between the land cover classes (Table 4).

For 2007, we only used the best performing classification algorithm from 2017 (SVM with a radial basis function kernel), which resulted in a similarly high overall accuracy of 93.4% (Table 3). We discovered that both SVM polynomial and RBF kernel classifiers in 2007 had similar classification results (Table 3). However, we chose the RBF because it had a higher producer's accuracy for mangrove (Table 3). Accuracies per class were similar to the 2017 classification. Surface water, urban regions, mangrove forests and agricultural lands were easily detected with producer's accuracy above 80% while Nipa Palm had a PA of 42%. This was because, Nipa Palm was mostly confused with mangrove forests (25% of classified pixels) and surface water (26%) (Table 5).

We also visually compared the different classification results (Figure 4). Across three regions where visual evidence was presence based on fieldwork: Calabar estuary with heavy Nipa Palm invasion (Figure 4a), Oproama community with no Nipa Palm invasion (Figure 4b) and Imo River Estuary with intact stands but medium invasion (Figure 4c). ML overestimated Nipa Palm vegetation, predicting its presence even in areas where they are non-existent. SVM classifiers performed better in separating Nipa Palm from mangrove and other LC classes, with its distribution matching the author's expectations from areas they have visited during the fieldwork, and based on the literature.

3.2. Classification Results

As stated above, we chose an optimal mapping method for 2007 and 2017 (SVM with RBF), and this represented the best LC maps for the Niger Delta (Figure 5). We estimated a mangrove area of 911,548 (895,781–927,315) ha and 1 441 (0–5742) ha Nipa Palm area in 2007; and 801,774 ha (±34,787; 95% Confidence Interval [CI]) mangrove area and Nipa Palm area of 11,447 ha (±7343; 95% CI) in 2017 (Table 6). In 2007, Cross River had the lowest mangrove area (28,154 ha) and Delta state had the highest mangrove area (290,797 ha). The lowest Nipa Palm area was observed in Rivers state (86 ha) and highest Nipa Palm area in Akwa Ibom (429 ha) in 2007. In 2017, lowest Nipa Palm (514 ha) and mangrove (24,478 ha) area in Cross River state while we estimated the highest mangrove cover (239,881 ha) in Bayelsa state and largest Nipa Palm (3746 ha) influence in Rivers state (Table 7). We also reported mangrove area based on the coastal division of Nigeria by Hughes and Hughes, (1992) [78] (Table 8).

We observed that mangrove forests extended about 60 km in the western Niger Delta basin (Delta state—Figure 5a). We also calculated a mangrove extent of 40 km in the central Niger Delta basin (Bayelsa State—Figure 5b); 60 km inland around the eastern Niger Delta basin (Rivers state—Figure 5c); 20 km in Imo River (Akwa Ibom state—Figure 5d) and about 3 km along the Cross River estuary (Figure 5e). We observed from the classification maps that agricultural lands were around settlements and rain forests close to river water shed (Figure 5f). Along the coast, we observed Nipa Palm fringes followed by a longer strip of mangrove forests before transitioning to tropical forests. We observed most of the Nipa Palm fringes along Imo river estuaries especially in Kono Creek and Ete Creek. These Nipa Palm fringes were also associated with urban settlements such as Opobo, Rivers State and Ikot Abasi, Akwa Ibom State (Figure 6).

Table 3. LC classification accuracy (%) of 2007 and 2017 for the classification types showing individual accuracies of the land cover classes (see Section 2.5).

Year	Classification Type (Number of Bands)	Kernel Type	Penalty Parameter	Overall Accuracy	Accuracy	Surface Water	Agricultural Land	Rain Forest	Mangrove Forest	Nipa Palm	Built Up Areas
2017	ML (4)	–	–	44.4%	PA	76	57	10	38	92	36
					UA	99	69	76	39	1	65
	(7)	–	–	66.8%	PA	83	94	13	55	98	92
					UA	99	94	92	48	3	89
	(10)	–	–	67.4%	PA	81	97	15	53	100	92
					UA	100	88	97	51	3	89
	(31 3 × 3 Occurrence Matrix)	–	–	77.0%	PA	81	99	56	65	100	89
					UA	100	75	91	82	5	92
	(31 7 × 7 Occurrence Matrix)	–	–	76.9%	PA	79	100	50	62	100	98
					UA	100	82	99	79	4	88
	SVM (31)	Linear	100	93.0%	PA	94	98	89	90	13	98
					UA	94	97	87	92	33	95
			50	92.5%	PA	94	98	89	90	5	98
					UA	93	98	87	91	33	95
		RBF	100	92.9%	PA	94	99	89	89	32	98
					UA	94	98	86	93	30	95
		Polynomial	100	92.8%	PA	94	99	89	88	32	98
					UA	94	97	86	93	30	95
2007	SVM (31)	RBF	100	93.4%	PA	99	94	82	97	42	95
					UA	96	95	98	85	63	95
		Polynomial	100	93.4%	PA	99	94	82	97	38	95
					UA	96	95	98	85	65	95

PA: Producer's Accuracy; UA: User's Accuracy; ML: Maximum Likelihood; SVM: Support Vector Machine; RBF: Radial Basis Function.

Table 4. Confusion Matrix of the 2017 SVM Radial Basis Function kernel Land Cover Classification of the Niger Delta.

			Ground Truth (Pixels)				
Class	**Surface Water**	**Agricultural Land**	**Rain Forest**	**Mangrove Forest**	**Nipa Palm**	**Built Up Areas**	**Total**
Unclassified	0	0	0	0	0	0	0
surface water	2408	1	5	98	25	20	2557
agricultural land	0	2821	67	2	0	2	2892
rain forest	38	15	2085	252	0	24	2414
mangrove forest	106	0	113	3057	17	1	3294
Nipa Palm	2	0	2	42	20	0	66
built up areas	8	27	66	2	0	1906	2009
Total	2562	2864	2338	3453	62	1953	13,232
			Ground Truth (Percent)				
Class	**Surface Water**	**Agricultural Land**	**Rain Forest**	**Mangrove Forest**	**Nipa Palm**	**Built Up Areas**	**Total**
Unclassified	0	0	0	0	0	0	0
surface water	93.99	0.03	0.21	2.84	40.32	1.02	19.32
agricultural land	0	98.5	2.87	0.06	0	0.1	21.86
rain forest	1.48	0.52	89.18	7.3	0	1.23	18.24
mangrove forest	4.14	0	4.83	88.53	27.42	0.05	24.89
Nipa Palm	0.08	0	0.09	1.22	32.26	0	0.5
built up areas	0.31	0.94	2.82	0.06	0	97.59	15.18
Total	100	100	100	100	100	100	100

Table 5. Confusion Matrix of the 2007 SVM Radial Basis Function kernel Land Cover Classification of the Niger Delta.

			Ground Truth (Pixels)				
Class	**Surface Water**	**Agricultural Land**	**Rain Forest**	**Mangrove Forest**	**Nipa Palm**	**Built Up Areas**	**Total**
Unclassified	0	0	0	0	0	0	0
surface water	3175	1	0	83	14	25	3298
agricultural land	3	5419	35	1	1	226	5685
rain forest	16	31	3440	31	0	1	3,519
mangrove forest	18	59	696	4701	13	23	5510
Nipa Palm	0	0	0	13	22	0	35
built up areas	4	267	1	13	3	5601	5889
Total	3216	5777	4172	4842	53	5876	23,936
			Ground Truth (Percent)				
Class	**Surface Water**	**Agricultural Land**	**Rain Forest**	**Mangrove Forest**	**Nipa Palm**	**Built Up Areas**	**Total**
Unclassified	0	0	0	0	0	0	0
surface water	98.73	0.02	0.00	1.71	26.42	0.43	13.78
agricultural land	0.09	93.80	0.84	0.02	1.89	3.85	23.75
rain forest	0.50	0.54	82.45	0.64	0.00	0.02	14.70
mangrove forest	0.56	1.02	16.68	97.09	24.53	0.39	23.02
Nipa Palm	0.00	0.00	0.00	0.27	41.51	0.00	0.15
built up areas	0.12	4.62	0.02	0.27	5.66	95.32	24.60
Total	100	100	100	100	100.00	100	100

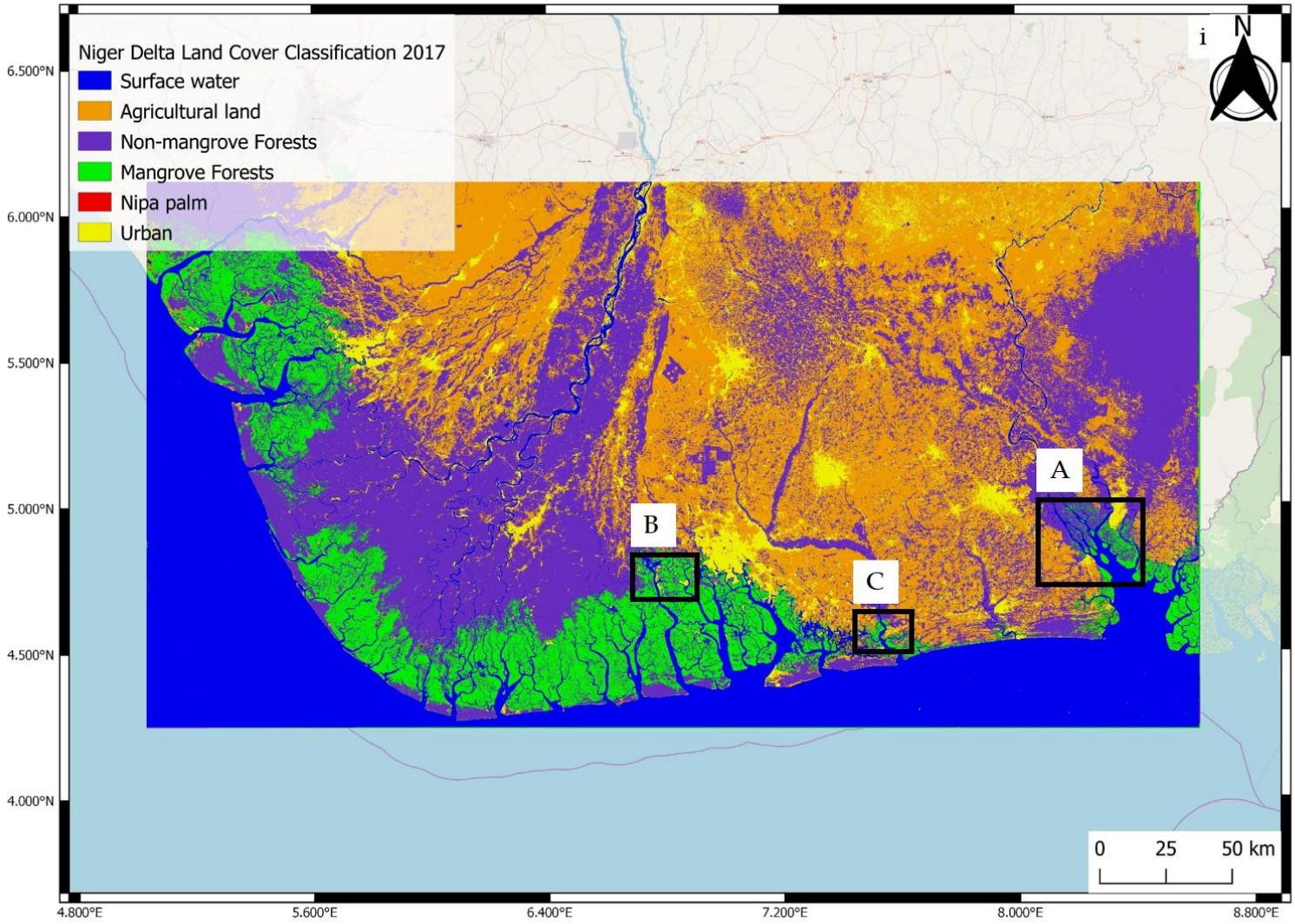

Figure 4. *Cont.*

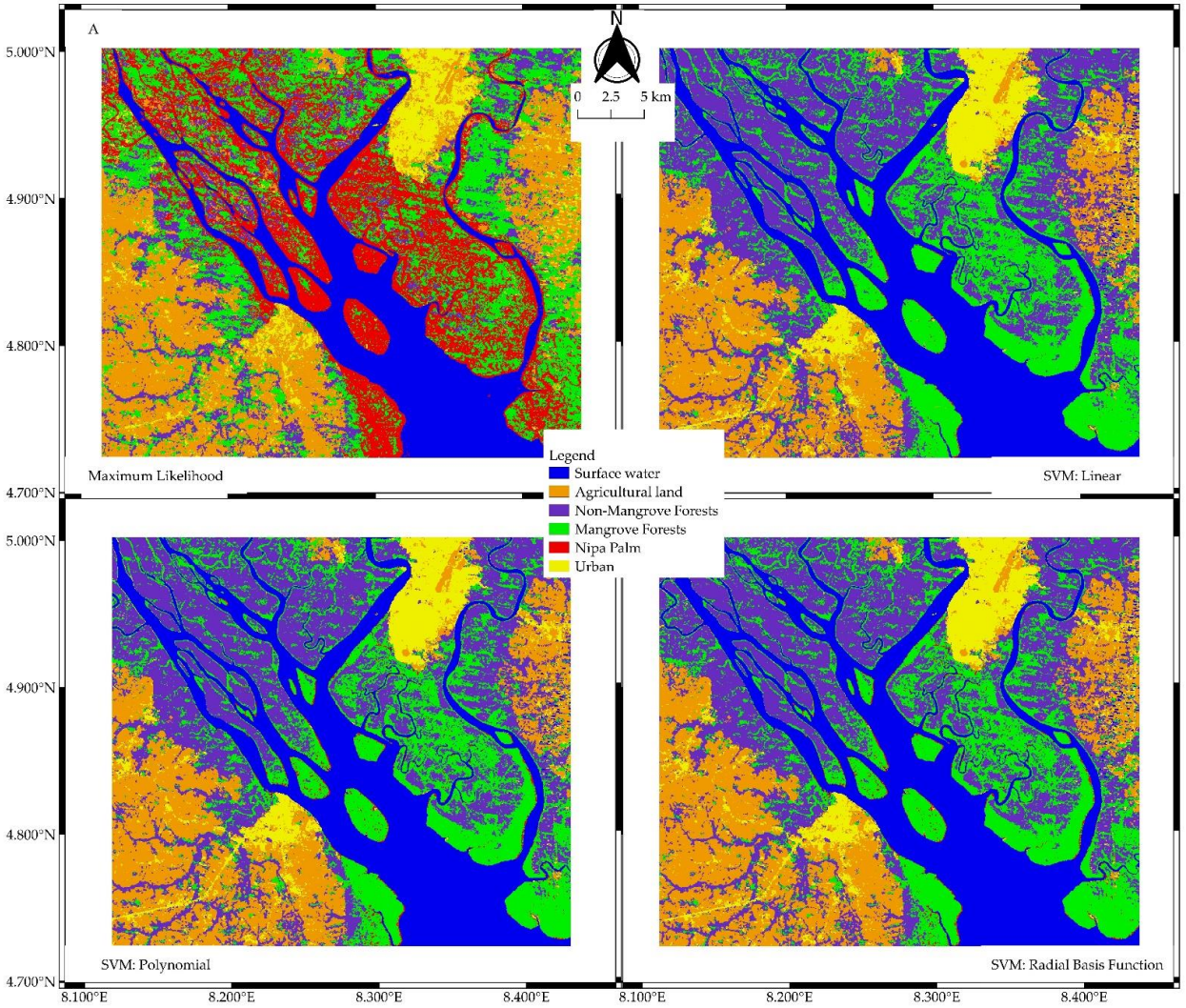

Figure 4. *Cont.*

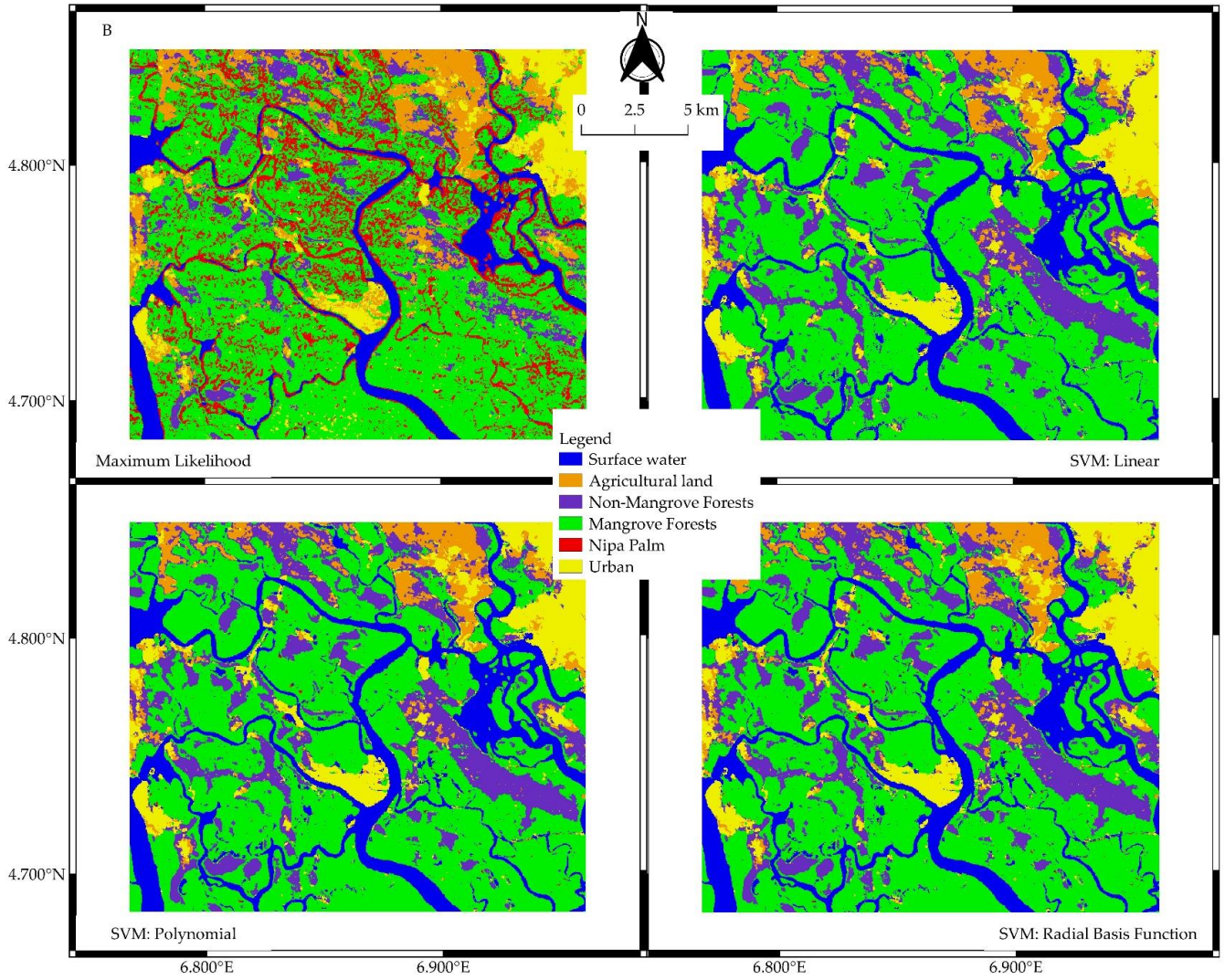

Figure 4. *Cont.*

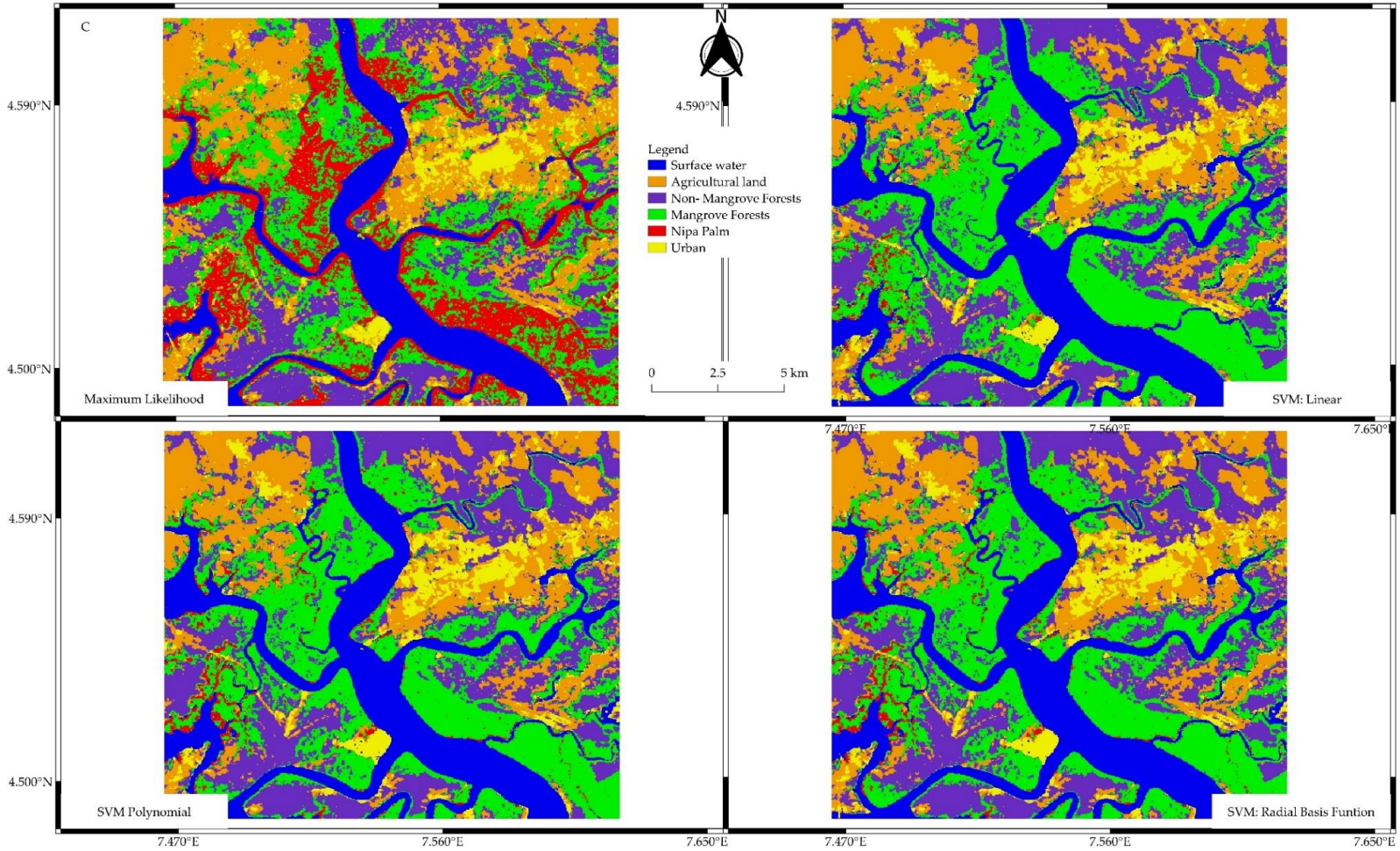

Figure 4. 2017 thematic map from Support Vector machine: Radial Basis Function kernel type (**i**) highlighting inset regions. Detailed analysis of the thematic maps produced by the different classifiers (Maximum Likelihood, Support Vector machine: Linear, Polynomial and Radial Basis Function kernel types) in three regions of the Niger Delta (Support Vector machine: Radial Basis Function): (**A**) Calabar Estuary; (**B**) Oproama Community and (**C**) Imo River Estuary.

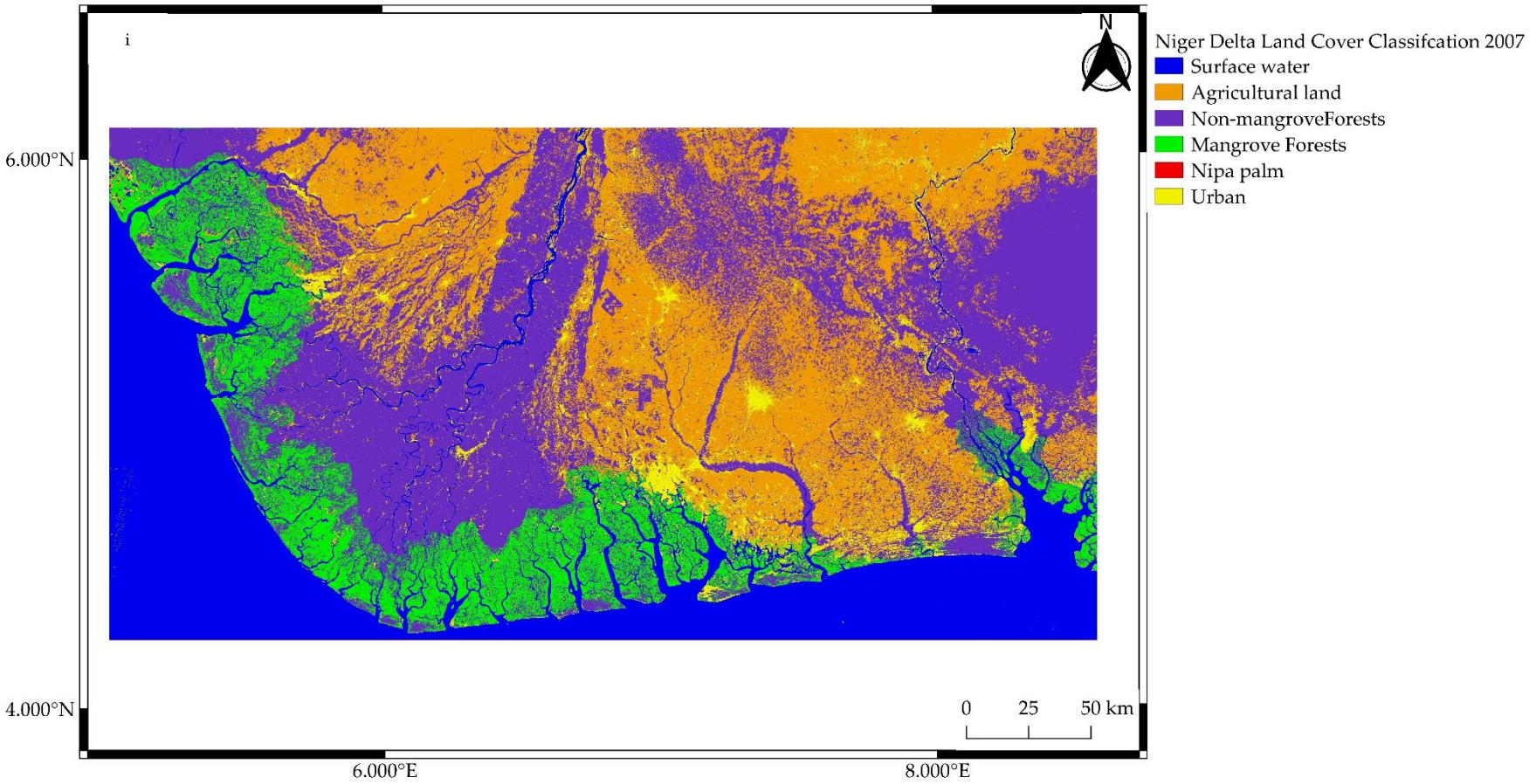

Figure 5. *Cont.*

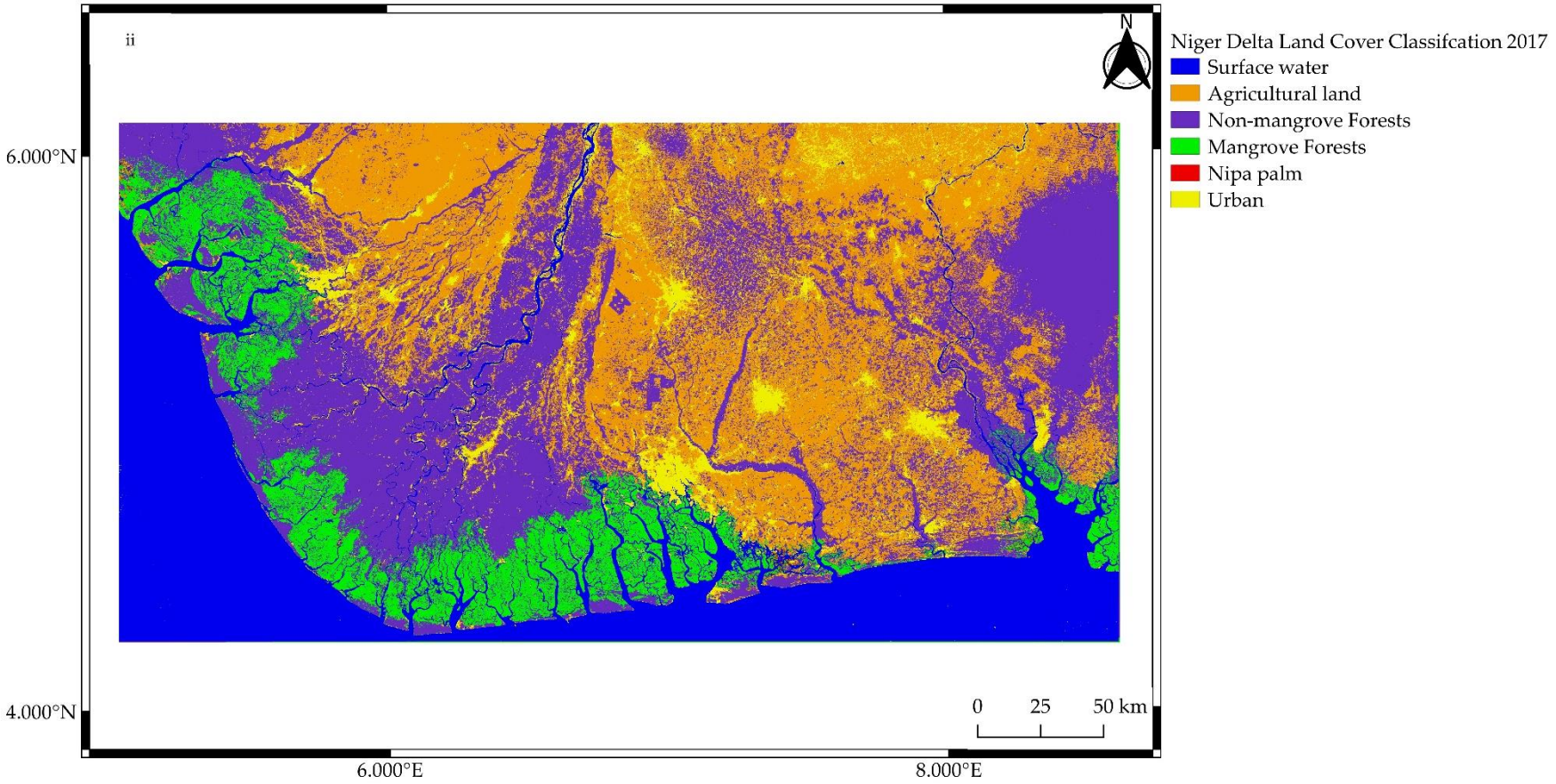

Figure 5. *Cont.*

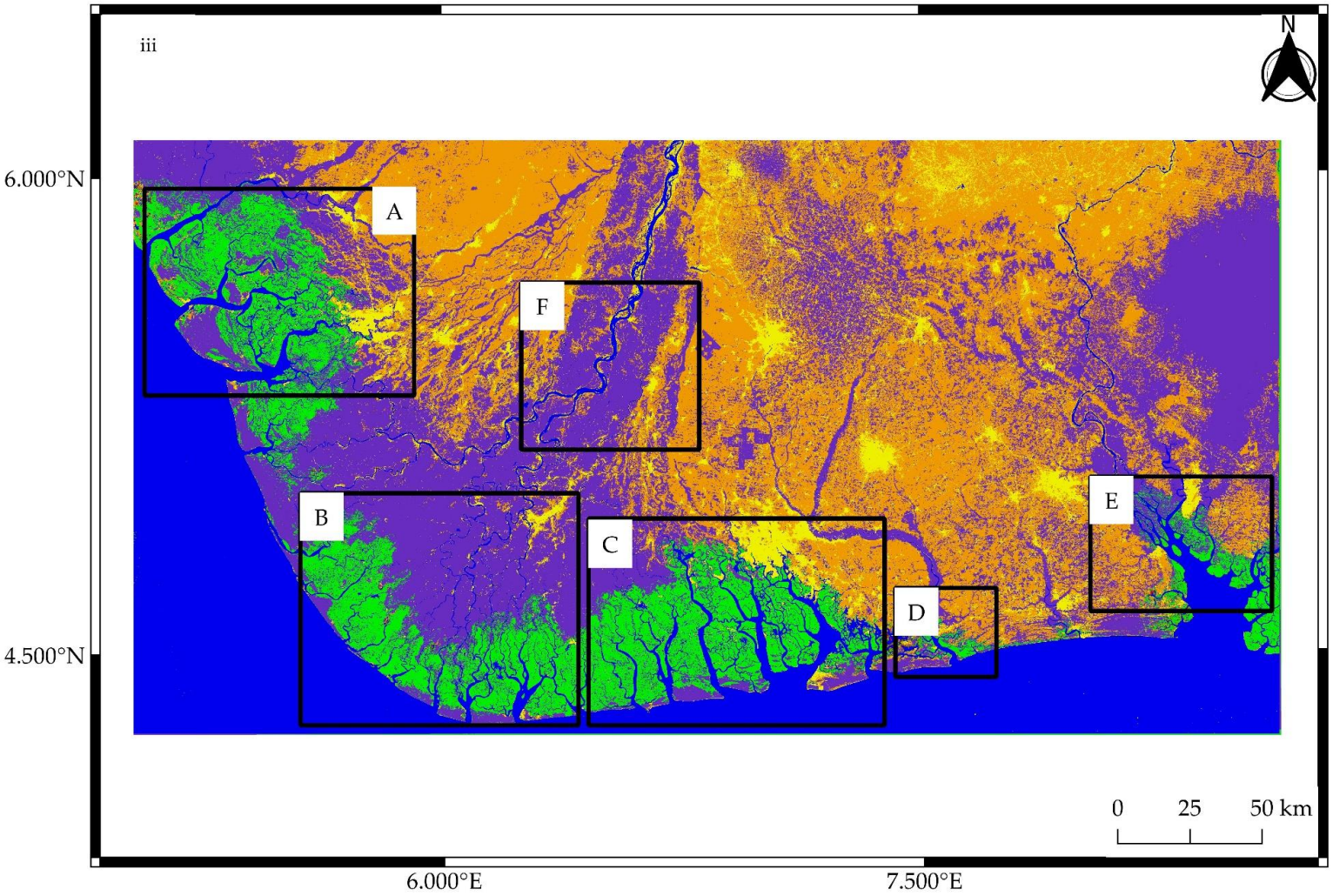

Figure 5. *Cont.*

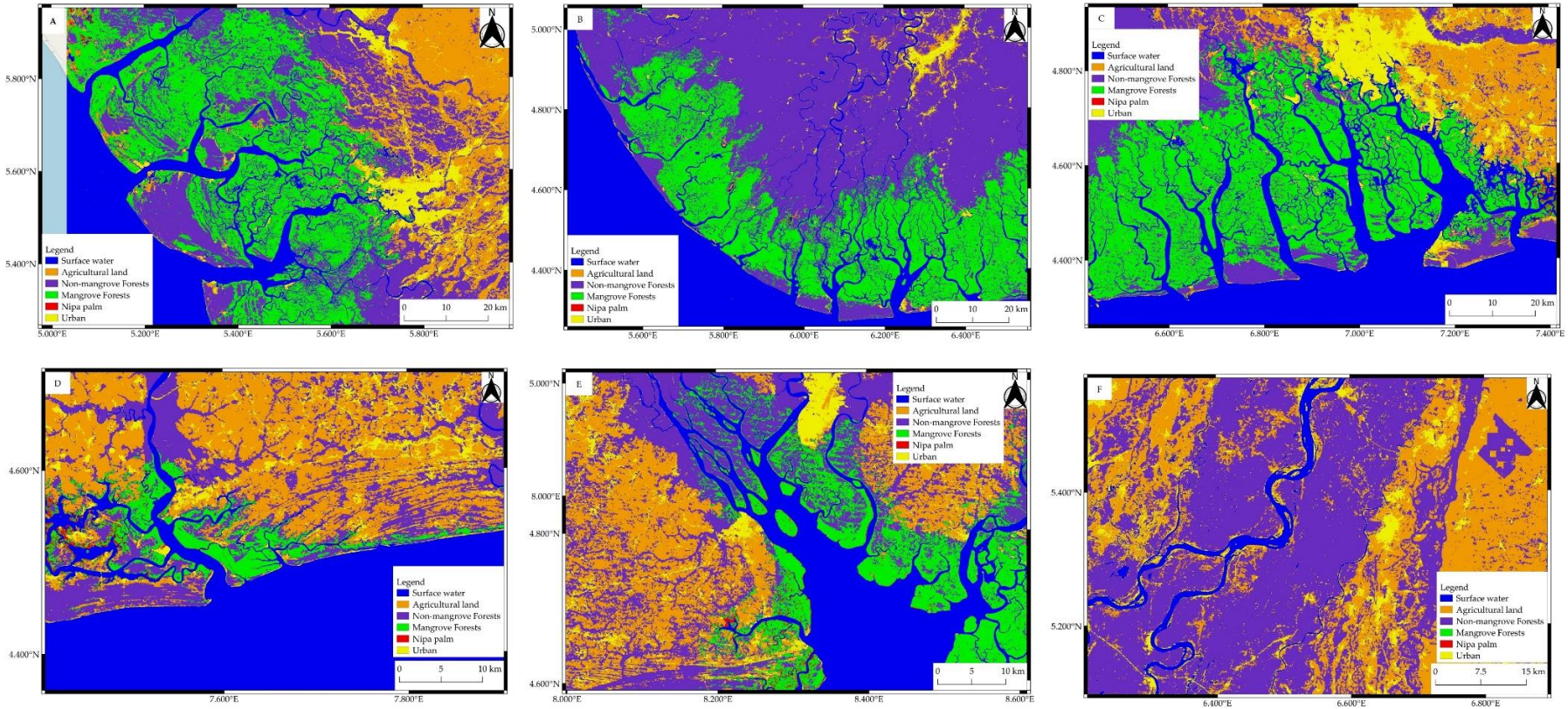

Figure 5. 2007 (**i**) and 2017 (**ii**) thematic map derived from the classification of layer stacked SRTM DEM, ALOS PALSAR, and Landsat 7 of the Niger Delta using SVM with Radial Basis Function Kernel. Inset (**iii**) shows the inland extent of mangrove forests from the 2017 classification in (**A**) western Niger Delta; (**B**) central Niger Delta; (**C**) eastern Niger Delta; (**D**) Imo River estuary; (**E**) Calabar estuary; and (**F**) the River Niger Basin bifurcation and the spread of surface water proximity to rain forests and agricultural land surrounding urban settlements.

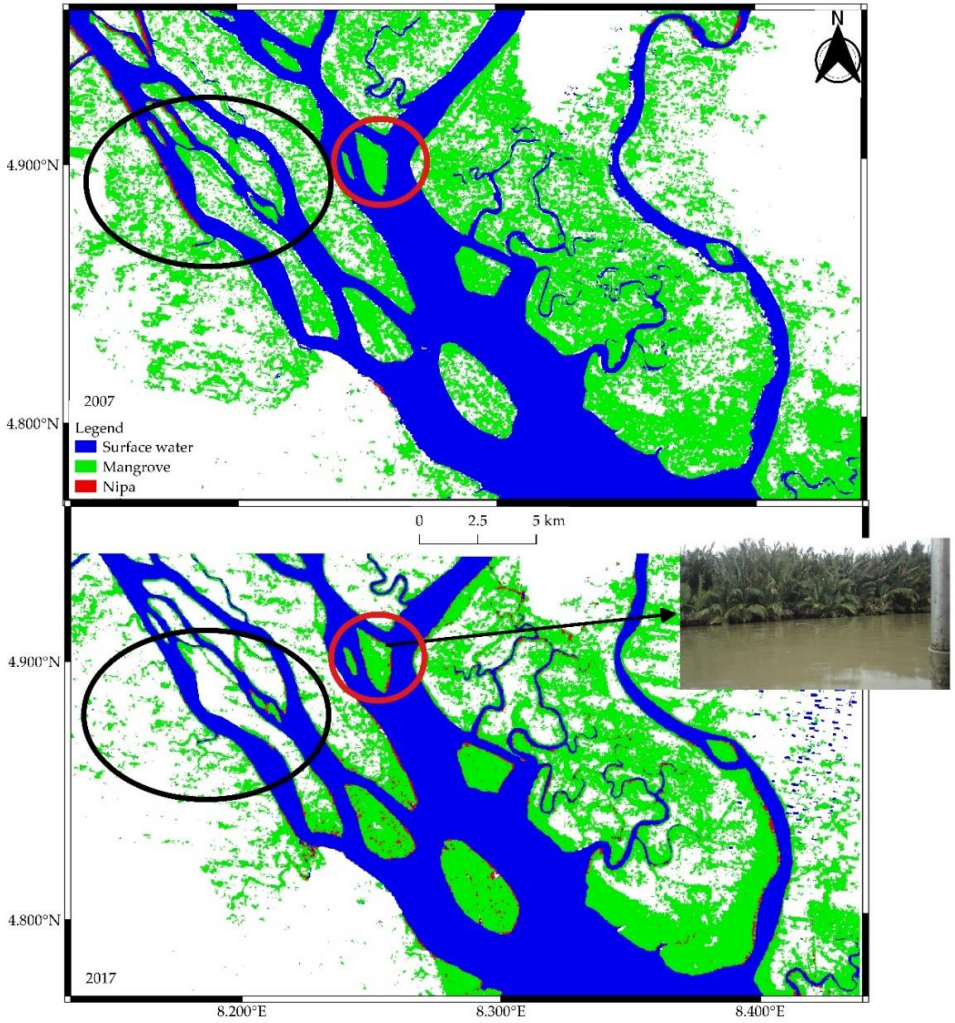

Figure 6. Mangrove forests loss along islands off the coast of Akwa Ibom and nipa palm colonization in Alligator Island, Calabar River Estuary of the Niger Delta. Black circles represent mangrove loss while red circles represent Nipa Palm colonization. Inset pictures of study sites during GCP selection.

Table 6. Change Detection analysis Using SVM–RBF kernel for each Land cover between 2007 and 2017 over the Study Area. Land cover class areas reported with 95% confidence interval in bracket.

Land Cover Classes	2007		2017		2017–2007	
	Area (ha)	Area (%)	Area (ha)	Area (%)	Change (ha)	Change (%)
Agricultural land	2,173,317 (2,158,427–2,189,005)	34.11	2,417,929 (2,401,778–2,434,080)	37.9	−244,213 (212,773–275,653)	11 (10–13)
Tropical Forest	2,889,083 (2,872,245–2,905,921)	45.35	2,549,919 (2,511,832–2,588,006)	40.0	339,164 (284,239–394,089)	−12 (10–14)
Mangrove forest	911,548 (895,781–927,315)	14.31	801,774 (766,987–836,561)	12.6	109,774 (59,221–160,327)	−12 (7–17)
Nipa palm	1441 (0–5742)	0.02	11,444 (4101–18,787)	0.2	−10,003 (−1641–18,787)	694 (−29–1304)
Built up areas	394,985 (382,299–407,671)	6.21	593,759 (580,375–607,143)	9.3	−198,774 (172,704–224,844)	50 (45–55)

Table 7. Area of Mangrove and Nipa Palm in Niger Delta States and Change in Land Cover Classes from 2007 and 2017 over the region.

Nigerian State	Mangrove Area (ha)			Nipa Palm Area (ha)		
	2017	2007	Change (%)	2017	2007	Change (%)
Akwa Ibom	27,853	31,888	−4034 (−13)	2414	429	1986 (463)
Bayelsa	239,881	284,840	−44,960 (−16)	1225	167	1059 (635)
Cross River	24,478	28,154	−3676 (−13)	514	269	245 (91)
Delta	238,697	290,797	−52,100 (−18)	2930	322	2608 (809)
Rivers	236,234	252,468	−16,234 (−6)	3746	86	3660 (4263)

Table 8. Mangrove and Nipa Palm Extent across Coastal Divisions of Coastal Nigeria.

Coastal Division	Mangrove Area (ha)			Nipa Area (ha)		
	2017	2007	Change (%)	2017	2007	Change (%)
Cross River Estuary	48,680	52,866	−4187 (−8)	2911	669	2242 (335)
Niger Delta basin	722,321	844,187	−121,867 (−14)	8256	634	7622 (1203)

3.3. Change Detection of Mangrove and Nipa Area

Comparing the two final maps, there was a 12% (range 10–14%) loss in forest over the entire delta and an increase of 11% in agricultural land (range 10–13%) and 50% in urban regions (range 45–55%) (Table 6). There was a 12% decrease in mangrove area (range 7–17%) and a likely large increase in Nipa Palm area (600%), but with large uncertainty (range 29–1304%) between 2007 and 2017 (Table 4). We observed that ~50% of Nipa Palm area in 2017 invaded mangrove forests (Figure 7) and ~6% of mangroves were converted to farmlands or urban regions. The largest relative decrease in mangrove area was in Delta state (18%) and the lowest decrease in Rivers state (6%) (Table 7). The highest Nipa Palm increase was also observed in Rivers state. Based on the coastal division by Hughes and Hughes, (1992) [78]; we observed an 8% loss of mangrove area at the Cross River estuary and 14% loss in the Niger Delta basin (Table 8).

We also analyzed the loss of mangrove and Nipa Palm spread over some local regions notably Benin River, Imo River and Calabar estuary (Figure 6). There was a 15% reduction in mangrove area and over fivefold increase of Nipa Palm area in the Benin River estuary. Imo river estuary had a 40% decrease in mangrove area with over 50% of Nipa Palm colonization from these regions. We recorded a reduction of 9% in mangrove area in the third region along the Calabar estuary.

3.4. Comparison with Global Mangrove Datasets

We compared our regional map to global maps (Figure 8) generated by Giri et al., 2010, Spalding et al., 2010 and the Global Mangrove Watch [10,11,79,80]. Data for comparison were acquired using the UN Ocean Data Viewer [81]. It is important to note that these maps were from different years (Table 9) and represents mangrove forests area in Nigeria. We compared two regions along the Niger Delta, Oproama Creek (Figure 8a) and Benin River estuary (Figure 8b) in our study and the maps generated by the GMW showing similarity in mangrove forests in the Niger Delta. This similarity could be possibly because of similar datasets used. However, there were some underestimation in some regions from the GMW compared to this study, which may have been due to unavailability of ground control points. We also showed a trend in Nipa Palm invasion in the Calabar estuary (Figure 8c) by comparing the global maps from different years. The maps shows a clear replacement of mangrove forests by Nipa Palm.

Table 9. Comparison of Mangrove Area estimated by Global Datasets.

	This Study	GMW 2010	Giri et al. 2011	Spalding et al. 2010
Mangrove Area (ha)	801,774 (766,987–836,561)	695,800	622,373	713,000
Date/range	2017	2010	1997–2000	1999–2003

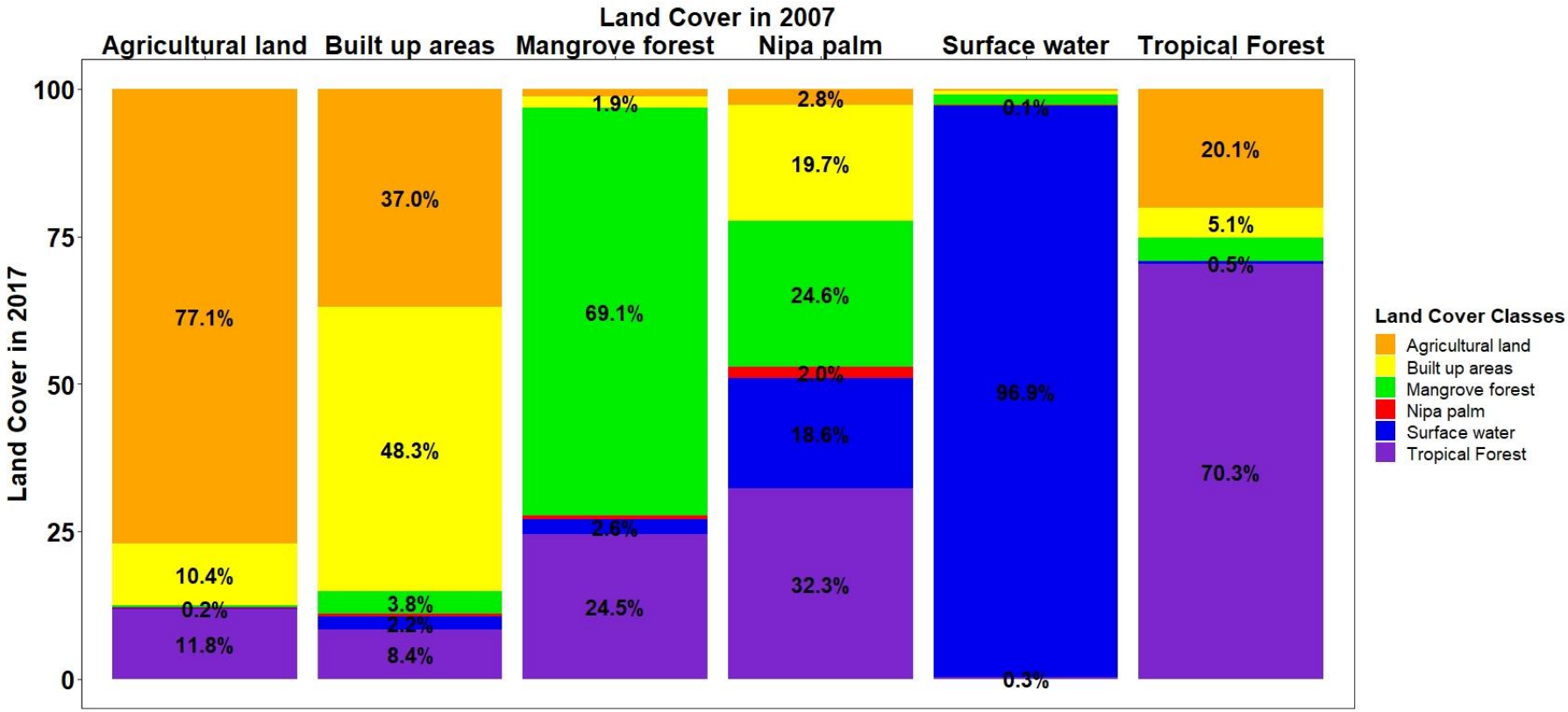

Figure 7. Percentage change of land cover classes in the Niger Delta between 2007 and 2017.

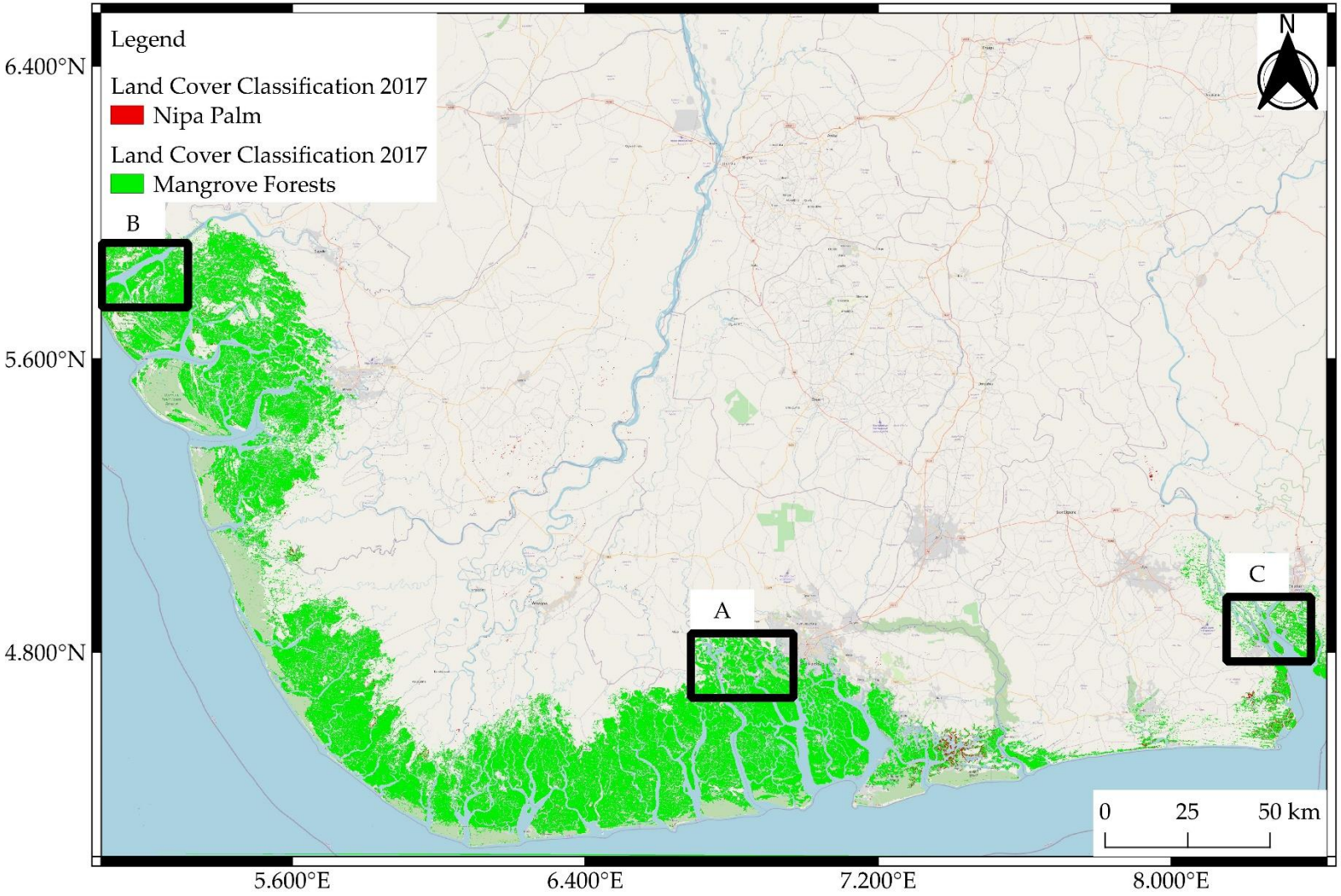

Figure 8. *Cont.*

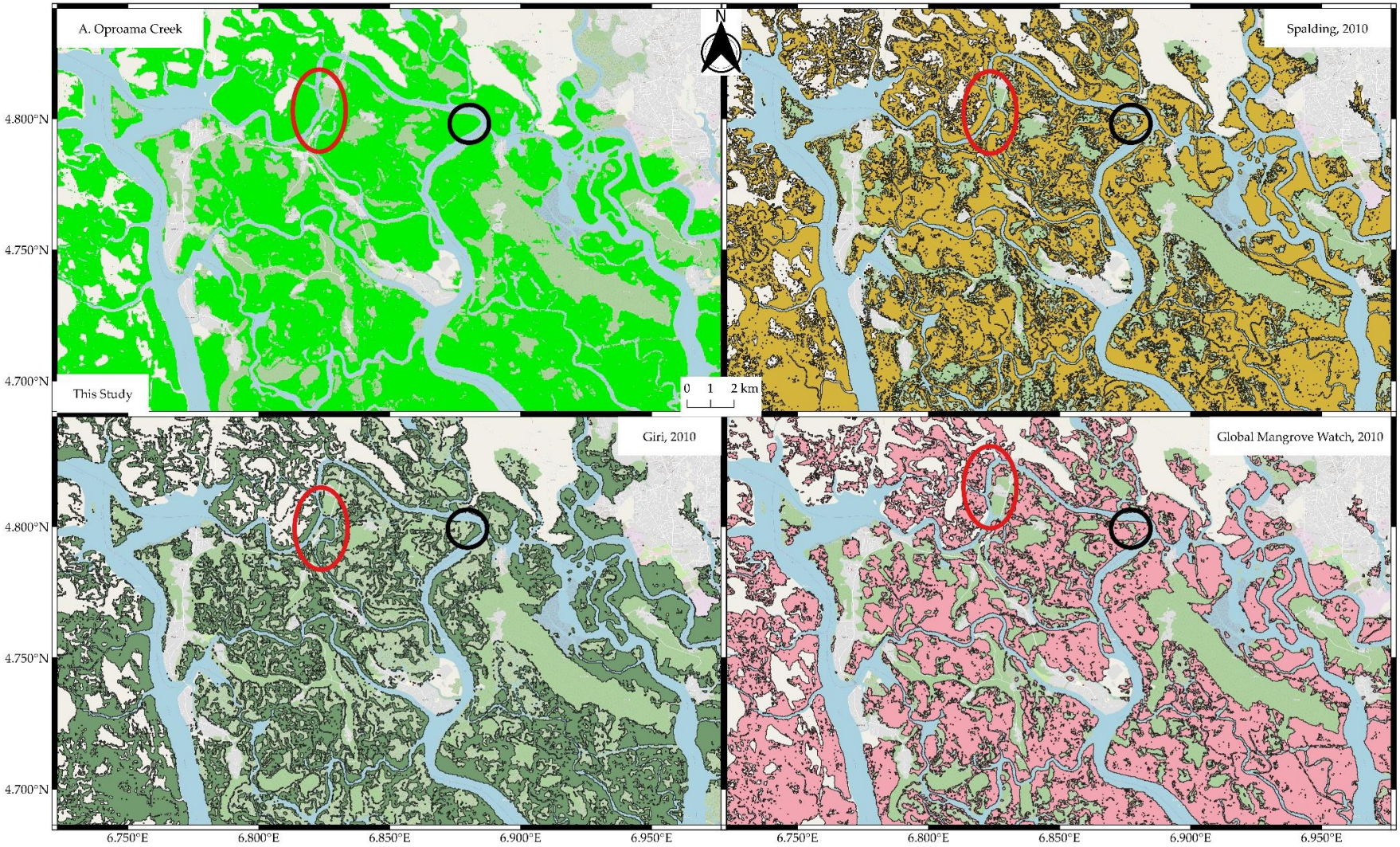

Figure 8. *Cont.*

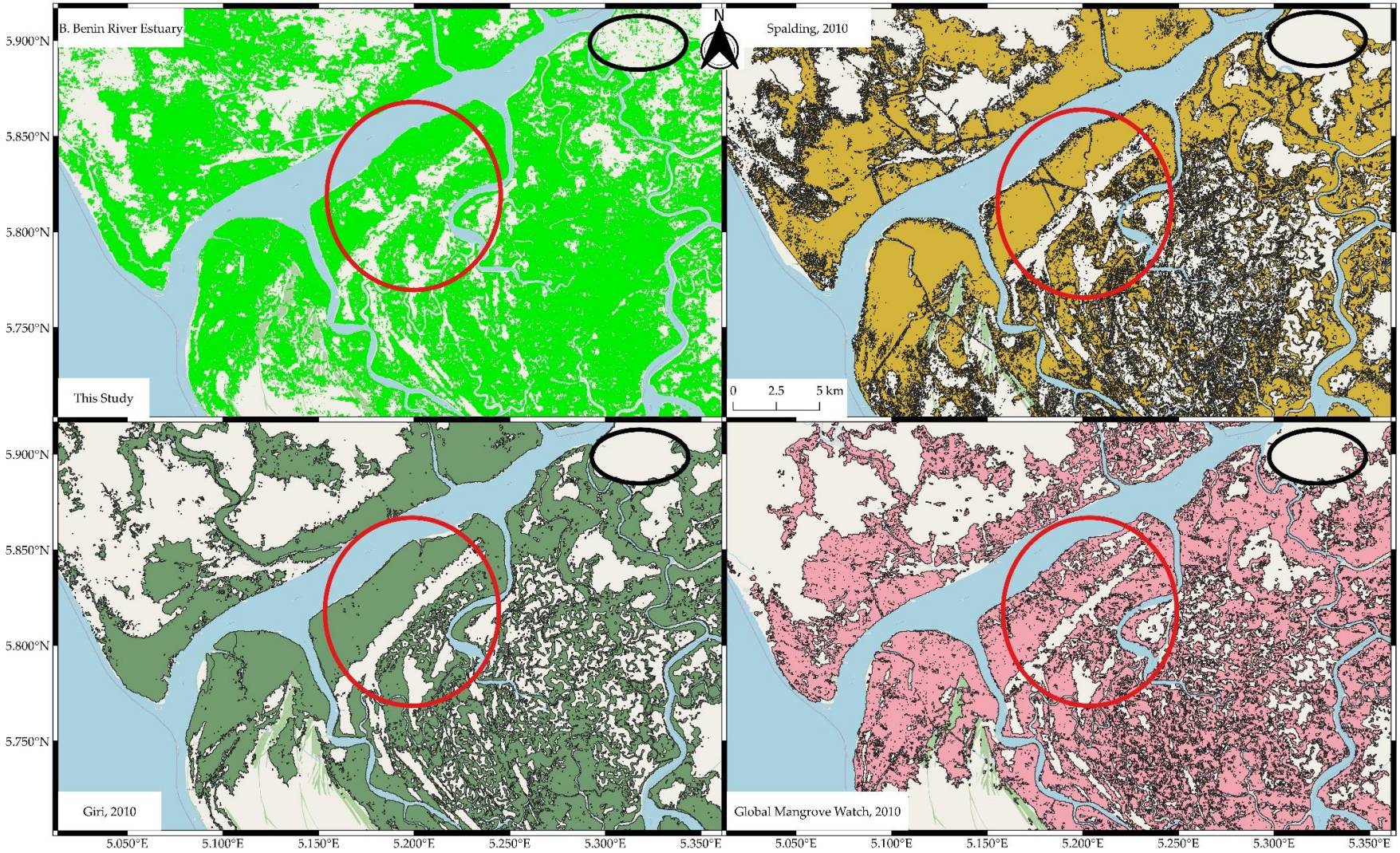

Figure 8. *Cont.*

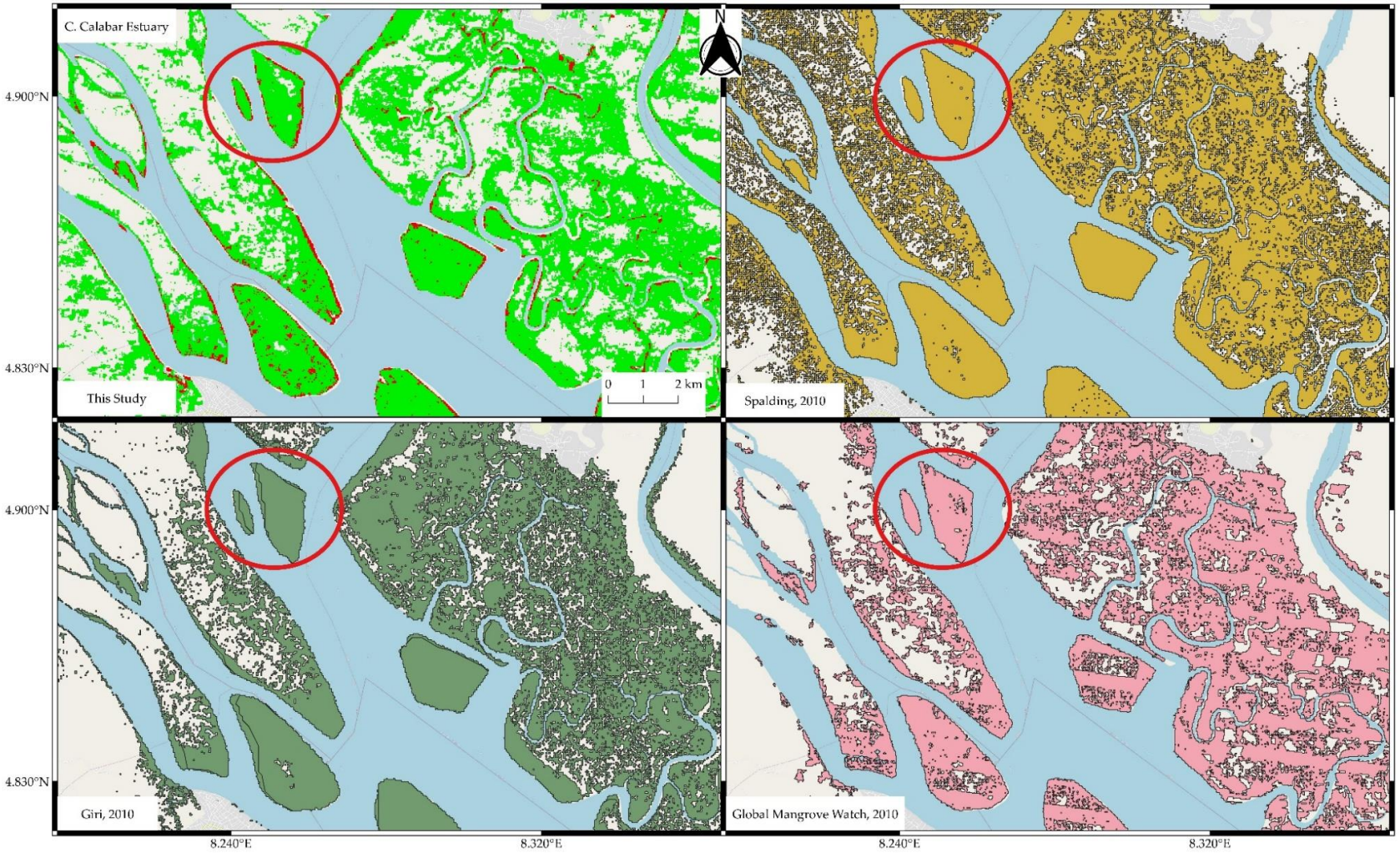

Figure 8. Comparison of different mangrove maps with red circles showing similarities and black circles showing underestimation. (**A**) Oproama creek; (**B**) Benin river estuary; and (**C**) Calabar estuary showing Nipa Palm cover on Alligator Island compared with global maps.

4. Discussion

We produced the first LC classification of the Niger Delta based on comprehensive ground data, to estimate mangrove and Nipa Palm cover and recent changes. We used both radar and optical imagery [39] and compared the accuracy of different types of classification algorithms to effectively classify these land cover types. Our results show that the Niger Delta has nearly a million hectares of mangroves, itself more than any other country in Africa [82], and previous global studies may have underestimated mangrove forest area in Nigeria. However, we also found rapid changes are occurring, with a decrease in mangrove area and likely rapid increase in the invasive Nipa Palm from 2007 to 2017.

4.1. Comparison of Classifier Performance

The classification results showed the SVM has a better ability to classify LC in this region than LMC using these datasets. This is not surprising, as the SVM classifier has been known to outperform ML [83] in other areas because it allows a more complex separation plane between classes [43]. SVM creates a multi-dimensional plane which allows for a separation boundary to be established amongst classes [73]. Huang (2002) [43] reported that SVM had a more stable overall accuracy over ML, ANN, and DT [43]. We observed similar trend where ML had the lower classification overall accuracy and for the individual classes (Table 3). SVM has been reportedly used in the classification of mangrove forests [84] and invasive species [85]. The danger of this more sophisticated type of classifier is that it can over fit, by learning the characteristics of the training data to increase apparent accuracies, but perform worse against test data.

The urban area and water classes had uniformly high accuracy. This easy detection could be due to spectral nature of the classes (quite different to the vegetation classes of the rest of the images), and the inclusion of DEM which takes into account the height of these classes above sea level. We found the lowest accuracy was the Nipa Palm, which again is not surprising. Nipa Palm is spectrally quite similar to forest and mangrove, but further occurs as a thin fringe along mangrove forests and hence its spectral qualities are mixed with those of mangroves at the 30 m resolution of our classification. Difficulty in classifying vegetation ecotones was reported by [86] when classifying vegetation in muddy tidal flats [86]. Hence, importance in detecting ecotones can improve accuracy of classifications. Field surveys showed mature mixed stands of mangrove and Nipa Palm, causing even more difficulties for the classifier (Figure 9). As there is no clear hard border between Nipa Palm and mangroves, trying to produce a binary classification into two classes will always cause errors. Secondly, the fringe nature of Nipa Palm created a large percentage of confusion with surface water (Tables 4 and 5). This confusion is because of the tidal nature of coastal vegetation which can interfere with both optical and radar satellite data. In order to improve our classification accuracy, we applied texture measures on the radar and optical data, theorizing that the uniform height and composition of dense Nipa Palm stands compared to mangrove forests would have smoother textural characteristics than mangroves [87]. The combination of multiple explanatory bands, which explained Nipa Palm structure and difference in canopy structure to mangrove forests, improved the classification accuracy. However, significant errors remain likely due in part because the textural windows (7×7 pixels) are larger than the normal patch size of the vegetation types, meaning pure statistics were rare.

A further issue peculiar to coastal regions is the tide: changing water levels can cause misclassification of Nipa Palm, mangrove and surface waters as the water level differs at the time of remote sensing data acquisition. This issue is compounded by different sources of satellite imagery with different sensing times, which can increase uncertainties in spatial characteristics and result in biased maps [88]. Ideally, all imagery should be collected at a particular point in the tide cycle (e.g., low tide), but the lack of data (both radar and cloud-free optical) made this selection impossible: we had to use what was available.

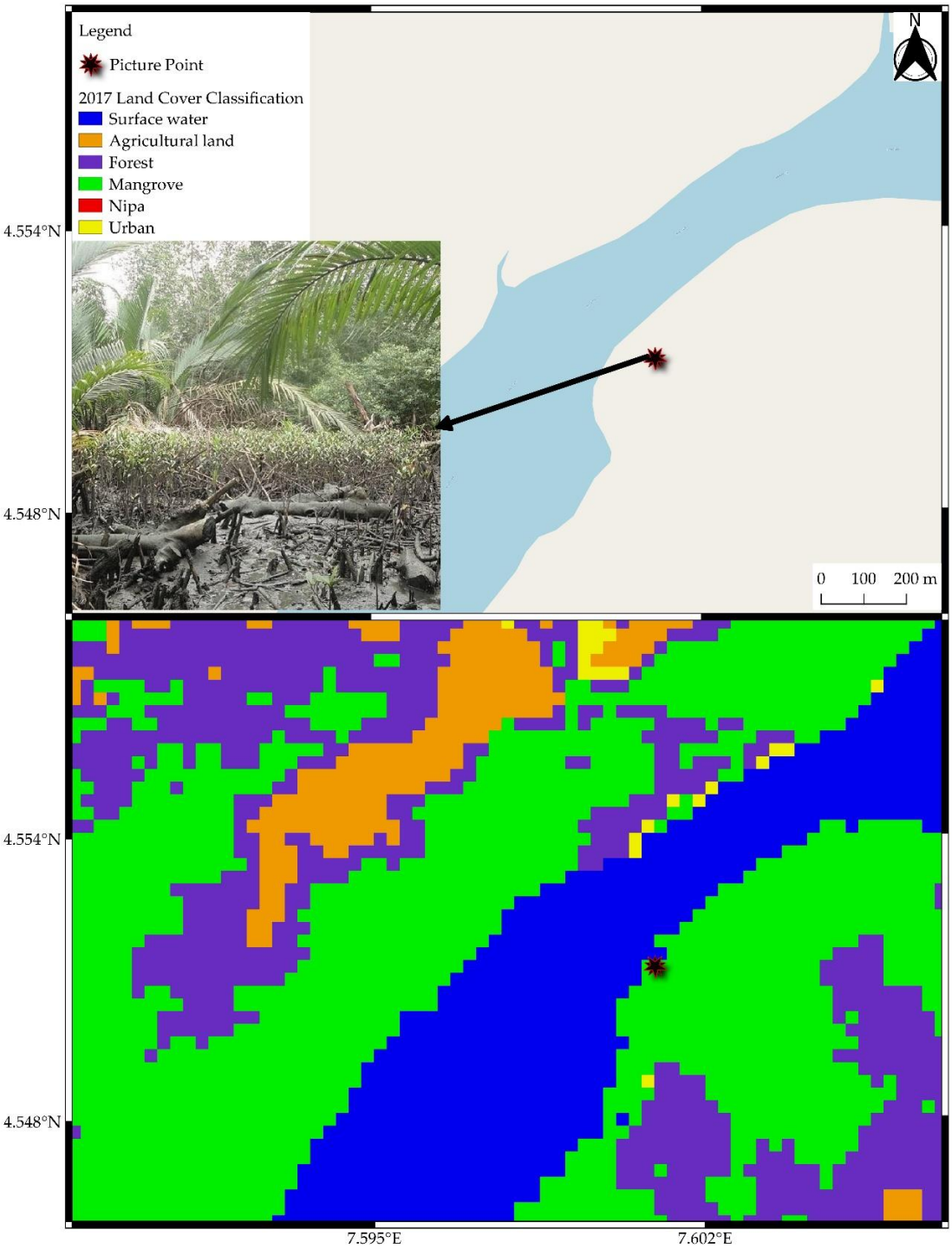

Figure 9. Mixed stand of Nipa Palm and disturbed mangrove in Ete creek.

4.2. Current Mangrove and Nipa Palm Extent

Mangrove and Nipa Palm area from this study are comparable to past studies. Our estimates of mangroves area in the Niger Delta (801,774 ha) is ~14% higher than those reported by Bunting et al., (2018) [11]. The relatively large variation in reports of mangrove area regionally and globally are a result of the methodology used in land cover classification (Table 7). The various reports of mangrove area regionally and globally will naturally contain errors in this area as they are based on global algorithms and ground data. We believe the differences in area was particularly caused by the landward extent of mangrove forests from the coast, which is high in Nigeria, possibly higher than average: this is an important threshold in mangrove classification that varies regionally. Our results show similarities with the land ward extent of mangroves from Spalding et al., (1997) [9] especially in the central Niger Delta [9]. We therefore conclude that mangrove area in Nigeria (and also the rate of Nigeria's mangrove area loss) has been underestimated by global datasets.

The global mangrove maps mirrored the spatial extent of mangrove forests in the Niger Delta (Figure 7). We observed that more than 90% of Nigerian mangroves lie within the core Niger Delta states of Delta, Bayelsa and Rivers states. This coverage was also reported by Fatoyinbo and Simard, (2013) reporting about 80% of mangroves lie within the Niger Delta swamps [50]. The ability of regional maps to estimate the presence of mangrove patches could also be a reason of the differences in globally reported mangrove area. The utilization of >500 GCPs during our study aided in the identification of mangrove patches which may have been undetected due to generalization. The landward extent of mangrove forests is an important threshold in mangrove classification as they vary regionally; GCPs are likely important in fixing this boundary. Thomas et al. (2018) [14] reported a 25.9% larger estimate in Riau region, Indonesia, due to a greater estimate on mangrove landward margin. They also attributed the higher estimate to mangrove gain [14]. Landward expansion has also been reported by Suyadi et al. (2019) [89] in Auckland, New Zealand, sometimes at the expense of salt marshes [89].

Nipa Palm distribution in Nigeria has a long and interesting historical record. Spalding et al., (1997) [9] reported that in the Palaeocene era, *Nypa* pollen had fossil records in both Nigeria and Brazil. Hence, Nipa Palm has always been associated with the Atlantic coasts. However, none was likely there in 1906 when it was introduced exotically for beautification and beach erosion [23]. We recorded Nipa Palm cover of about 11,000 ha, though with high uncertainty, with the largest recorded in both the Calabar estuary and the eastern Niger Delta. These two regions have had Nipa Palm introduced in 1906 [23] at Calabar estuary and in the 1960s at the Imo River estuary [90]. Our results show a similar trend with reducing Nipa Palm cover along an east to west gradient. We recorded lower Nipa Palm cover than those recorded by Isebor et al. (2003) [26], recording a 82,100 ha cover in 2003 [26]. Despite being an underestimate of previous reports and wide range of uncertainty, more research is needed to have a more accurate estimate to facilitate management of Nipa Palm. Understanding the trend in invasive species spread can help manage the conservation of native species in an ecosystem.

4.3. Change Detection

Urbanization, oil pollution and unsustainable exploitation of wood products are the major causes of mangrove deforestation in Nigeria. We recorded a 12% loss of mangrove and tropical forests over the decade, which could have been because of population dependent factors such as pollution, urbanization, agricultural expansion and Nipa Palm invasion [21]. This conversion rate shows the influence of population growth on forest resources in the Niger Delta, with pressure on land areas and food resources increasing. The Niger Delta region had a population of 30 million in 2005 but this is projected to almost double, currently estimated with a population of about 45 million in 2020 [16]. The increasing population has been described as an ecological time bomb especially in Rivers state [91]. Hence, there will be increasing the demand for available land for development and agriculture. The increasing urbanization in the Delta could have possible effects on mangrove cover. Infrastructural development at the expense of mangrove regions in the delta threatens the biodiversity of this carbon rich ecosystem [92]. The replacement of mangrove regions in the Niger Delta could also be because

of hydrographic modifications in the Niger delta due to dredging activities [49]. The widening and deepening of canals in creeks can modify the estuarine properties in which mangrove forests thrive.

We reported a likely 10-fold increase in Nipa Palm from 1441 ha in 2007 to 11,444 ha in 2017 with a range of a gain of 1641 ha to a loss of 18,787 ha. Nipa proliferation was greater in mangrove-cleared areas. The likely large increase in Nipa Palm was mostly at the expense of mangrove forest: ~50% of the Nipa Palm area in our analysis was from the loss of mangrove cover in the region, especially in Akwa Ibom state. This non-native invasive species colonize structurally matured native species through disturbance or a pattern of penetrating mangrove stands (Figure 9). Our confidence intervals also show a possible reduction in Nipa Palm area (29%; 1641 ha) and possibly no change. These possible error in change detection could be a baseline for further investigation of invasive species in Niger Delta mangrove forests.

4.4. Caveats and Limitations

We encountered the problem of creating training classes for Nipa Palm classification, because Nipa Palm occurs in a strip along mangrove fringes, which only go some, meters inland. However, the fine resolution of the sensors (30 m) assisted as this could account for a larger coverage especially in areas of heavy colonization. Future research can take into account finer scale remote sensing products. Our results also show low accuracy in classifying Nipa Palm evident from the low Producer and User's accuracies (Table 3). Care should be taken when interpreting these results.

Cloud cover was also a limitation in using Landsat imagery for land cover analysis. Cloudiness had an effect on the clarity of optical data which is visible in our classification results over the Niger Delta (Figure 10), and scan line (SLC-off) error from the Landsat equipment movement affecting some of the regions during the classification [11]. Over the mangrove forests estimated in both years, there was no cloud influence in 2007 and 1.8% in 2017. Future regional classification of mangrove forests can make use of air-borne instruments on airplanes while Nipa Palm differentiation can make use of drones. These instruments will be able to account for finer optical characteristics of coastal vegetation that can improve accuracy.

We used image texture measures to increase the identification of major land cover classes especially agriculture lands and forests that spans large areas. Non-inclusion of these texture measures resulted in lower classification accuracies (Table 3). However, the use of texture measures probably reduced the map resolution, further hindering the accuracy of Nipa Palm classification which occurs as thin strips. Future land cover classification for identification of invasive species occupying thin strips could make use of finer scale resolution, which will improve the effectiveness of image texture.

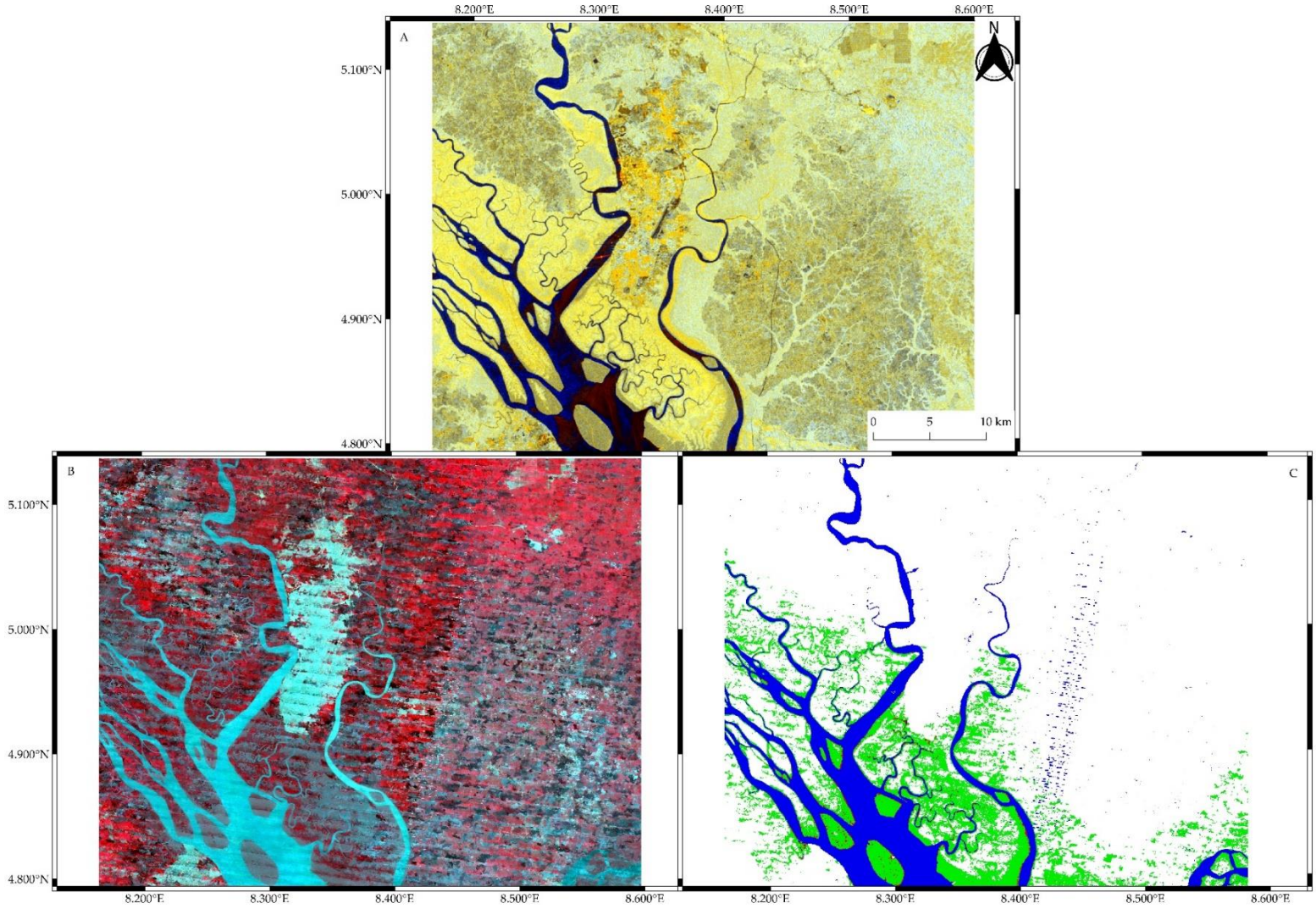

Figure 10. Cloud cover limitation of Optical data over Kwa Ibo river southeastern Nigeria. (**A**) ALOS PALSAR radar scene; (**B**) classification imagery; (**C**) infrared scene.

5. Conclusions

Using a combination of EO data and ground control points, mangrove forests of the Niger Delta can be effectively monitored. We showed that mangrove forests in the Niger Delta cover a larger area, and stretch further inland, than was known previously. However, we also show that the area of mangrove forests is decreasing fast, through conversion to agriculture or urban areas, and through the proliferation of the invasive Nipa Palm.

Our best results involved direct observations and texture data from optical and SAR data, combined with a DEM, and analyzed using the SVM method. In general, our 95% confidence intervals, based on independent test data, were narrow enough for confident conclusions on area change to be drawn. However, classifying Nipa Palm poses a challenge, with no method producing reliable classifications with accuracies for this class over 32%. Our results therefore provide a foundation for monitoring the vegetation of the Niger Delta, but monitoring of Nipa Palm might require a higher resolution method.

The results have shown opportunities for monitoring and management of mangrove forests in the Niger Delta. Nipa Palm in the Niger Delta is a non-resourceful invasive species, which, if not checked, will eradicate the valuable mangroves. Improved mapping precision can target areas with high incidence of logging, population growth and economic activity in order to generate a mangrove vulnerability map in the Niger Delta. Our results show that Nigeria is one of the top five ranked countries in the world in terms of mangrove forest area, and the first ranked in Africa, but this may be rapidly changing due to adverse effects from development, logging and sea level rise. Utilization of remote sensing products, which can provide a baseline in spatial and temporal analysis, can be the first step in national mangrove forests monitoring, protection and restoration plans.

Author Contributions: Conceptualization, C.N.; methodology, C.N., M.W., E.T.A.M.; software C.N.; validation, C.N., M.W., E.T.A.M.; formal analysis, C.N.,; investigation, C.N.; resources, C.N., M.W., E.T.A.M.; data curation, C.N.; writing—original draft preparation, C.N.; writing—review and editing, C.N., M.W., E.T.A.M.; visualization, C.N.; supervision, M.W., E.T.A.M.; project administration, C.N., M.W., E.T.A.M.; funding acquisition, C.N., M.W., E.T.A.M. All authors have read and agreed to the published version of the manuscript.

Funding: The Elizabeth Sinclair Irvine Bequest and Centenary Agroforestry 89 Fund from the University of Edinburgh funded the field component of this research. C.N. is supported by the Presidential Scholarship Scheme for Innovation and Development (PRESSID) of the Federal Ministry of Education, Nigeria. E.T.A.M.'s contribution to this study was part funded by NERC grant NE/R016860/1.

Acknowledgments: We would like to acknowledge the efforts of the fieldwork team in the Niger Delta: Goodluck, Davies, Major and Asuquo. I want to appreciate the Oproama, Kono, and Ete communities for ease of access to mangrove forests. The Global Change Ecology lab and Elizabeth Sinclair Forestry Funds supported this work. We would like to also acknowledge the financial support of the University of Edinburgh.

Conflicts of Interest: The authors declare no conflict of interest.

Appendix A

Table A1. Confusion Matrix of the 2017 SVM Polynomial kernel Land Cover Classification of the Niger Delta.

	Ground Truth (Pixels)						
Class	**surface water**	**agricultural land**	**rain forest**	**mangrove forest**	**Nipa Palm**	**built up areas**	**Total**
Unclassified	0	0	0	0	0	0	0
surface water	2404	1	6	104	26	21	2562
agricultural land	0	2822	70	2	0	1	2895
rain forest	38	15	2081	252	0	25	2411
mangrove forest	110	0	113	3050	16	1	3290
Nipa Palm	2	0	1	43	20	0	66
built up areas	8	26	67	2	0	1905	2008
Total	2562	2864	2338	3453	62	1953	13,232
	Ground Truth (Percent)						
Class	**surface water**	**agricultural land**	**rain forest**	**mangrove forest**	**Nipa Palm**	**built up areas**	**Total**
Unclassified	0	0	0	0	0	0	0
surface water	93.83	0.03	0.26	3.01	41.94	1.08	19.36
agricultural land	0	98.53	2.99	0.06	0	0.05	21.88
rain forest	1.48	0.52	89.01	7.3	0	1.28	18.22
mangrove forest	4.29	0	4.83	88.33	25.81	0.05	24.86
Nipa Palm	0.08	0	0.04	1.25	32.26	0	0.5
built up areas	0.31	0.91	2.87	0.06	0	97.54	15.18
Total	100	100	100	100	100	100	100

Table A2. Confusion Matrix of the 2017 ML Land Cover Classification of the Niger Delta.

	Ground Truth (Pixels)						
Class	**surface water**	**agricultural land**	**rain forest**	**mangrove forest**	**Nipa Palm**	**built up areas**	**Total**
Unclassified	0	0	0	0	0	0	0
surface water	2068	0	0	0	0	0	2068
agricultural land	16	2836	628	99	0	192	3771
rain forest	17	1	1312	103	0	3	1436
mangrove forest	158	1	315	2231	0	8	2713
Nipa Palm	265	0	10	1006	62	17	1360
built up areas	38	26	73	14	0	1733	1884
Total	2562	2864	2338	3453	62	1953	13,232
	Ground Truth (Percent)						
Class	**surface water**	**agricultural land**	**rain forest**	**mangrove forest**	**Nipa Palm**	**built up areas**	**Total**
Unclassified	0	0	0	0	0	0	0
surface water	80.72	0	0	0	0	0	15.63
agricultural land	0.62	99.02	26.86	2.87	0	9.83	28.5
rain forest	0.66	0.03	56.12	2.98	0	0.15	10.85
mangrove forest	6.17	0.03	13.47	64.61	0	0.41	20.5
Nipa Palm	10.34	0	0.43	29.13	100	0.87	10.28
built up areas	1.48	0.91	3.12	0.41	0	88.74	14.24
Total	100	100	100	100	100	100	100

References

1. Lugo, A.E.; Medina, E.; Wang, Y. Mangrove Forests. *Encycl. Nat. Resour. Land* **2014**, 343–352. [CrossRef]
2. Bouillon, S.; Borges, A.V.; Castañeda-Moya, E.; Diele, K.; Dittmar, T.; Duke, N.; Kristensen, E.; Lee, S.Y.; Marchand, C.; Middelburg, J.J.; et al. Mangrove production and carbon sinks: A revision of global budget estimates. *Glob. Biogeochem. Cycles* **2008**, *22*, 12. [CrossRef]
3. Kauffman, J.B.; Heider, C.; Cole, T.G.; Dwire, K.A.; Donato, D.C. Ecosystem Carbon Stocks of Micronesian Mangrove Forests. *Wetlands* **2011**, *31*, 343–352. [CrossRef]
4. Mcleod, E.; Salm, R.V. *Managing Mangroves for Resilience to Climate Change*; World Conservation Union (IUCN): Gland, Switzerland, 2006; Volume 64, ISBN 9782831709536.
5. Karmaker, S. Study of Mangrove Biomass, Net Primary Production & Species Distribution using Optical & Microwave Remote Sensing Data. Ph.D. Thesis, Indian Institute of Remote Sensing, Dehradun, India, 2006.
6. Richards, D.; Friess, D.A. Rates and drivers of mangrove deforestation in Southeast Asia, 2000–2012. *Proc. Natl. Acad. Sci. USA* **2015**, *113*, 344–349. [CrossRef] [PubMed]
7. Akanni, A.; Onwuteaka, J.; Uwagbae, M.; Mulwa, R.; Elegbede, I.O. The Values of Mangrove Ecosystem Services in the Niger Delta Region of Nigeria. In *The Political Ecology of Oil and Gas Activities in the Nigerian Aquatic Ecosystem*; Elsevier BV: Amsterdam, The Netherlands, 2018; pp. 387–437.
8. Hamdan, O.; Aziz, H.K.; Hasmadi, I.M. L-band ALOS PALSAR for biomass estimation of Matang Mangroves, Malaysia. *Remote Sens. Environ.* **2014**, *155*, 69–78. [CrossRef]
9. Spalding, M.; Blasco, F.; Field, C. *World Mangrove Atlas, Version 3*; Routledge: Okinawa, Japan, 1997.
10. Giri, C.; Ochieng, E.; Tieszen, L.L.; Zhu, Z.; Singh, A.; Loveland, T.; Mašek, J.; Duke, N. Status and distribution of mangrove forests of the world using earth observation satellite data. *Glob. Ecol. Biogeogr.* **2010**, *20*, 154–159. [CrossRef]
11. Bunting, P.; Rosenqvist, A.; Lucas, R.; Rebelo, L.-M.; Hilarides, L.; Thomas, N.; Hardy, A.; Itoh, T.; Shimada, M.; Finlayson, C. (Max) The Global Mangrove Watch—A New 2010 Global Baseline of Mangrove Extent. *Remote Sens.* **2018**, *10*, 1669. [CrossRef]
12. Worthington, T.; Spalding, M. *Mangrove Restoration Potential A Global Map Highlighting A Critical Opportunity Critical Opportunity*; Cambridge University: Cambridge, UK, 2018; p. 36.
13. Thomas, N.; Lucas, R.; Bunting, P.; Hardy, A.; Rosenqvist, Å.; Simard, M. Distribution and drivers of global mangrove forest change, 1996–2010. *PLoS ONE* **2017**, *12*, e0179302. [CrossRef]
14. Thomas, N.; Bunting, P.; Lucas, R.; Hardy, A.; Rosenqvist, A.; Fatoyinbo, T.L. Mapping Mangrove Extent and Change: A Globally Applicable Approach. *Remote Sens.* **2018**, *10*, 1466. [CrossRef]
15. Food and Agriculture and Organization The world's mangrove 1980–2005. *FAO For. Pap.* **2007**, *153*, 89.
16. NDDC Niger Delta Region Land and People. In *Niger Delta Regional Development Masterplan*; Printing Development Company Limited: Port Harcourt, Nigeria, 2006; pp. 48–99.
17. Omoregie, U. Nigeria's Petroleum Sector and GDP: The Missing Oil Refining Link. *J. Adv. Econ. Financ.* **2019**, *4*, 4. [CrossRef]
18. Adekola, O.; Mitchell, G. The Niger Delta wetlands: Threats to ecosystem services, their importance to dependent communities and possible management measures. *Int. J. Biodivers. Sci. Ecosyst. Serv. Manag.* **2011**, *7*, 50–68. [CrossRef]
19. Ndidi, C.; Okonkwo, P.; Kumar, L.; Taylor, S. The Niger Delta wetland ecosystem: What threatens it and why should we protect it? *Afr. J. Environ. Sci. Technol.* **2015**, *9*, 451–463.
20. Mmom, P.C.; Arokoyu, S.B. Mangrove forest depletion, biodiversity loss and traditional resources management practices in the Niger Delta, Nigeria. *Res. J. Appl. Sci. Eng. Technol.* **2010**, *2*, 28–34.
21. Numbere, M.M.A.O. Mangrove Habitat Loss and the Need for the Establishment of Conservation and Protected Areas in the Niger Delta, Nigeria. In *Habitats of the World—Biodiversity and Threats*; IntechOpen: Rijeka, Croatia, 2019; p. 13.
22. Hawthorne, T.L.; Elmore, V.; Strong, A.; Bennett-Martin, P.; Finnie, J.; Parkman, J.; Harris, T.; Singh, J.; Edwards, L.; Reed, P. Mapping non-native invasive species and accessibility in an urban forest: A case study of participatory mapping and citizen science in Atlanta, Georgia. *Appl. Geogr.* **2015**, *56*, 187–198. [CrossRef]

23. Ukpong, I.E. *Nypa fruticans* Invasion and the Integrity of Mangrove Ecosystem Functioning in the Marginal Estuaries of South Eastern Nigeria. In *Frontiers in Environmental Research and Sustainable Environment in the 21st Century*; Gbadegesin, A., Orimoogunje, O.O.I., Fashae, O.A., Eds.; Ibadan University Press Publishing House: Ibadan, Nigeria, 2015; pp. 1–13.
24. Okugbo, O.T.; Usunobun, U.; Adegbegi, J.A.; Okiemien, C.O. A review of Nipa Palm as a renewable energy source in Nigeria. *Res. J. Appl. Sci. Eng. Technol.* **2012**, *4*, 2367–2371.
25. UNEP. *Environmental Assessment of Ogoniland*; UNEP: Athens, Greece, 2011; ISBN 9789280731309.
26. Isebor, C.E.; Ajayi, T.O.; Anyanwu, A. The Incidence of *Nypa fruticans* (WURMB) and It's Impact on Fisheries Production in the Niger Delta Mangrove Ecosystem. In Proceedings of the 16th Annual Conference of the Fisheries Society of Nigeria (FISON), Maiduguri, Nigeria, 4–9 November 2001; pp. 13–16.
27. Langeveld, J.W.A.; Delany, S. The Impact of Oil Exploration, Extraction and Transport on Mangrove Vegetation and Carbon Stocks in Nigeria. Amsterdam, 2014. Available online: http://biomassresearch.eu/?mdocs-file=249 (accessed on 24 April 2016).
28. Hossain, F.; Islam, A. Utilization of Mangrove Forest Plant: Nipa Palm (*Nypa fruticans* Wurmb.). *Am. J. Agric. For.* **2015**, *3*, 156. [CrossRef]
29. Tsuji, K.; Sebastian, L.S.; Ghazalli, M.N.F.; Ariffin, Z.; Nordin, M.S.; Khaidizar, M.I.; Dulloo, M.E. Biological and ethnobotanical characteristics of Nipa Palm (*Nypa fructicans* wurmb.): A review. *Sains Malays.* **2011**, *40*, 1407–1412.
30. Bioresources Development and Conservation Programme (BDCP). *Assessment of Control Measures for Nypa Palm Infestation in Nigeria*; Bioresources Development and Conservation Programme (BDCP): Vienna, Austria, 2007.
31. Myint, S.W.; Giri, C.P.; Wang, L.; Zhu, Z.; Gillette, S.C. Identifying Mangrove Species and Their Surrounding Land Use and Land Cover Classes Using an Object-Oriented Approach with a Lacunarity Spatial Measure. *GIScience Remote Sens.* **2008**, *45*, 188–208. [CrossRef]
32. Lucas, R.M.; Mitchell, A.L.; Armston, J. Measurement of forest above ground biomass using active and passive remote sensing at large (country and continental) scales. *For. Rep. Rev.* **2015**, *1*, 162–177.
33. Fatoyinbo, T.E.; Armstrong, A.H. Remote Characterization of Biomass Measurements: Case Study of Mangrove Forests. In *Biomass*; Momba, M.N.B., Ed.; Books on Demand: Norderstedt, Germay, 2010; pp. 65–78. ISBN 9789533071138.
34. Fatoyinbo, T.; Simard, M. *Remote Sensing of Mangrove Structure and Biomass. Work. Trop. Wetl. Ecosyst. Indones. Sci. Needs to Address Clim. Chang. Adapt. Mitigation. Sanur Beach Hotel. Bali 11–14th April*; NASA Jet Propulsion Laboratory: Pasadena, CA, USA, 2011; p. 5.
35. Li, X.; Yeh, A.; Liu, K.; Wang, S. Inventory of mangrove wetlands in the Pearl River Estuary of China using remote sensing. *J. Geogr. Sci.* **2006**, *16*, 155–164. [CrossRef]
36. Lucas, R.; Mitchell, A.L.; Rosenqvist, A.; Proisy, C.; Melius, A.; Ticehurst, C. The potential of L-band SAR for quantifying mangrove characteristics and change: Case studies from the tropics. *Aquat. Conserv. Mar. Freshw. Ecosyst.* **2007**, *17*, 245–264. [CrossRef]
37. Japan Aerospace Exploration Agency. Kyoto & Carbon Initiative. Available online: https://www.eorc.jaxa.jp/ALOS/en/top/kyoto_top.htm (accessed on 18 July 2018).
38. Green, E.P.; Clark, C.D.; Mumby, P.J.; Edwards, A.J.; Ellis, A.C. Remote sensing techniques for mangrove mapping. *Int. J. Remote Sens.* **1998**, *19*, 935–956. [CrossRef]
39. Joshi, N.; Baumann, M.; Ehammer, A.; Fensholt, R.; Grogan, K.; Hostert, P.; Jepsen, M.R.; Kuemmerle, T.; Meyfroidt, P.; Mitchard, E.T.A.; et al. A Review of the Application of Optical and Radar Remote Sensing Data Fusion to Land Use Mapping and Monitoring. *Remote Sens.* **2016**, *8*, 70. [CrossRef]
40. Mathur, A.; Foody, G.M. Land cover classification by support vector machine: Towards efficient training. In Proceedings of the 2004 IEEE International Geoscience and Remote Sensing Symposium Proceedings, Anchorage, AK, USA, 20–24 September 2004; pp. 742–744. [CrossRef]
41. Deilmai, B.R.; Bin Ahmad, B.; Zabihi, H. Comparison of two Classification methods (MLC and SVM) to extract land use and land cover in Johor Malaysia. *IOP Conf. Series Earth Environ. Sci.* **2014**, *20*, 12052. [CrossRef]

42. Madanguit, C.J.G.; Oñez, P.J.L.; Tan, H.G.; Villanueva, M.D.; Ordaneza, J.E.; Aurelio, R.M.; Novero, A.U. Application of Support Vector Machine (SVM) and Quick Unbiased Efficient Statistical Tree (QUEST) Algorithms on Mangrove and Agricultural Resource Mapping using LiDAR Data Sets. *Int. J. Appl. Environ. Sci.* **2017**, *12*, 973–6077.
43. Huang, C.; Davis, L.S.; Townshend, J.R.G. An assessment of support vector machines for land cover classification. *Int. J. Remote Sens.* **2002**, *23*, 725–749. [CrossRef]
44. Heumann, B.W. An Object-Based Classification of Mangroves Using a Hybrid Decision Tree—Support Vector Machine Approach. *Remote Sens.* **2011**, *3*, 2440–2460. [CrossRef]
45. Szuster, B.W.; Chen, Q.; Borger, M. A comparison of classification techniques to support land cover and land use analysis in tropical coastal zones. *Appl. Geogr.* **2011**, *31*, 525–532. [CrossRef]
46. David, L.C.; Ballado, A.J. Mapping mangrove forest from LiDAR data using object-based image analysis and Support Vector Machine: The case of Calatagan, Batangas. In Proceedings of the 2015 International Conference on Humanoid, Nanotechnology, Information Technology, Communication and Control, Environment and Management (HNICEM), Cebu City, Philippines, 9–12 December 2015; pp. 1–5. [CrossRef]
47. Heumann, B.W. Satellite remote sensing of mangrove forests: Recent advances and future opportunities. *Prog. Phys. Geogr. Earth Environ.* **2011**, *35*, 87–108. [CrossRef]
48. Bradley, B.A. Accuracy assessment of mixed land cover using a GIS-designed sampling scheme. *Int. J. Remote Sens.* **2009**, *30*, 3515–3529. [CrossRef]
49. James, G.; Adegoke, J.O.; Saba, E.; Nwilo, P.; Akinyede, J. Satellite-Based Assessment of the Extent and Changes in the Mangrove Ecosystem of the Niger Delta. *Mar. Geodesy* **2007**, *30*, 249–267. [CrossRef]
50. Fatoyinbo, T.L.; Simard, M. Height and biomass of mangroves in Africa from ICESat/GLAS and SRTM. *Int. J. Remote Sens.* **2012**, *34*, 668–681. [CrossRef]
51. Bisgin, H.; Bera, T.; Ding, H.; Semey, H.G.; Wu, L.; Liu, Z.; Barnes, A.E.; Langley, D.A.; Pava-Ripoll, M.; Vyas, H.J.; et al. Comparing SVM and ANN based Machine Learning Methods for Species Identification of Food Contaminating Beetles. *Sci. Rep.* **2018**, *8*, 6532. [CrossRef] [PubMed]
52. Ukpong, I. Soil-vegetation interrelationships of mangrove swamps as revealed by multivariate analyses. *Geoderma* **1994**, *64*, 167–181. [CrossRef]
53. Ukpong, I.E. Gradient analysis in mangrove swamp forests. *Trop. Ecol.* **2000**, *41*, 25–32.
54. Ukpong, I.E. Ecological classification of Nigerian mangroves using soil nutrient gradient analysis. *Wetl. Ecol. Manag.* **2000**, *8*, 263–272. [CrossRef]
55. Aduloju, A.A.; Okwechime, I. Oil and Human Security Challenges in the Nigeria's Niger Delta. *Critique* **2016**, *44*, 505–525. [CrossRef]
56. Farr, T.G.; Rosen, P.A.; Caro, E.; Crippen, R.; Duren, R.; Hensley, S.; Kobrick, M.; Paller, M.; Rodríguez, E.; Roth, L.; et al. The Shuttle Radar Topography Mission. *Rev. Geophys.* **2007**, *45*, 45. [CrossRef]
57. SRTM. The Shuttle Radar Topography Mission (SRTM) Collection User Guide. 2015; pp. 1–17. Available online: https://lpdaac.usgs.gov/documents/179/SRTM_User_Guide_V3.pdf (accessed on 11 July 2019).
58. USGS Shuttle Radar Topography Mission. *1 Arc Second. Glob. L. Cover Facil. Univ. Maryland, Coll. Park. Maryland, Febr. 2000. 2004, Scenes: n0*; USGS: Lawrence, KS, USA, 2004.
59. Japan Aerospace Exploration Agency. ALOS-2 Overview. Available online: https://www.eorc.jaxa.jp/ALOS-2/en/about/overview.htm (accessed on 18 July 2018).
60. Japan Aerospace Exploration Agency. JAXA|Advanced Land Observing Satellite-2 (ALOS-2). Available online: http://www.jaxa.jp/projects/sat/alos2/index_e.html (accessed on 18 July 2018).
61. Shimada, M.; Ohtaki, T. Generating Large-Scale High-Quality SAR Mosaic Datasets: Application to PALSAR Data for Global Monitoring. *IEEE J. Sel. Top. Appl. Earth Obs. Remote Sens.* **2010**, *3*, 637–656. [CrossRef]
62. Gorelick, N.; Hancher, M.; Dixon, M.; Ilyushchenko, S.; Thau, D.; Moore, R. Google Earth Engine: Planetary-scale geospatial analysis for everyone. *Remote Sens. Environ.* **2017**, *202*, 18–27. [CrossRef]
63. *Exelis Visual Information Solutions*; L3Harris Geospatial: Boulder, CO, USA, 2010.
64. QGIS Development Team. QGIS Geographic Information System. Open Source Geospatial Foundation Project: 2018. Available online: https://qgis.org/en/site/ (accessed on 9 September 2018).
65. Google Earth Pro 2018. Available online: https://www.google.co.uk/earth/download/gep/agree.html (accessed on 9 September 2018).

66. *ESRI ArcGIS Desktop: Release 10*; Environmental Systems Research Institute: Redlands, CA, USA, 2011; Available online: http://www.esri.com/ (accessed on 9 September 2018).
67. Hansen, M.C.; Potapov, P.V.; Moore, R.; Hancher, M.; Turubanova, S.A.; Tyukavina, A. High-Resolution Global Maps of 21st-Century Forest Cover Change. *Science* **2013**, *342*, 850–853. [CrossRef] [PubMed]
68. Shimada, M.; Isoguchi, O.; Tadono, T.; Isono, K. PALSAR Radiometric and Geometric Calibration. *IEEE Trans. Geosci. Remote Sens.* **2009**, *47*, 3915–3932. [CrossRef]
69. Dewantoro, M.D.R.; Farda, N.M. ALOS PALSAR Image for Landcover Classification Using Pulse Coupled Neural Network (PCNN). *Int. J. Adv. Res. Comput. Eng.* **2012**, *1*, 289–294.
70. Lopes, A.; Touzi, R.; Nezry, E. Adaptive speckle filters and scene heterogeneity. *IEEE Trans. Geosci. Remote Sens.* **1990**, *28*, 992–1000. [CrossRef]
71. PCI Geomatics Radar Enhanced Lee Filter. Available online: http://www.pcigeomatics.com/geomatica-help/concepts/orthoengine_c/chapter_825.html (accessed on 22 May 2016).
72. Lee, J.-S. Digital Image Enhancement and Noise Filtering by Use of Local Statistics. *IEEE Trans. Pattern Anal. Mach. Intell.* **1980**, *2*, 165–168. [CrossRef] [PubMed]
73. Nanda, M.A.; Seminar, K.B.; Nandika, D.; Maddu, A. A Comparison Study of Kernel Functions in the Support Vector Machine and Its Application for Termite Detection. *Information* **2018**, *9*, 5. [CrossRef]
74. Karatzoglou, A.; Meyer, D.; Hornik, K. Support Vector Algorithm in R. *J. Stat. Softw.* **2006**, *15*, 1–28. [CrossRef]
75. Yang, X. Parameterizing Support Vector Machines for Land Cover Classification. *Photogramm. Eng. Remote Sens.* **2011**, *77*, 27–37. [CrossRef]
76. Congalton, R.G. A review of assessing the accuracy of classifications of remotely sensed data. *Remote Sens. Environ.* **1991**, *37*, 35–46. [CrossRef]
77. Olofsson, P.; Foody, G.M.; Herold, M.; Stehman, S.V.; Woodcock, C.E.; Wulder, M.A. Good practices for estimating area and assessing accuracy of land change. *Remote Sens. Environ.* **2014**, *148*, 42–57. [CrossRef]
78. Hughes, R.H.; Hughes, J.S. *A Directory of African Wetlands*, 34th ed.; IUCN: Gland, Switzerland; Cambridge, UK; UNEP: Nairobi, Kenya; WCMC: Cambridge, UK, 1992.
79. Krauss, K.W.; Friess, D.A. World Atlas of Mangroves. *Wetlands* **2011**, *31*, 1003–1005. [CrossRef]
80. Dahdouh-Guebas, F. World Atlas of Mangroves: Mark Spalding, Mami Kainuma and Lorna Collins (eds). *Hum. Ecol.* **2010**, *39*, 107–109. [CrossRef]
81. Schlitzer, R. Ocean Data View. 2018. Available online: https://data.unep-wcmc.org/ (accessed on 20 November 2018).
82. Hamilton, S.E.; Casey, D. Creation of a high spatio-temporal resolution global database of continuous mangrove forest cover for the 21st century (CGMFC-21). *Glob. Ecol. Biogeogr.* **2016**, *25*, 729–738. [CrossRef]
83. Kavzoglu, T.; Colkesen, I. A kernel functions analysis for support vector machines for land cover classification. *Int. J. Appl. Earth Obs. Geoinf.* **2009**, *11*, 352–359. [CrossRef]
84. Chance, C.M.; Coops, N.C.; Plowright, A.A.; Tooke, T.R.; Christen, A.; Aven, N. Invasive Shrub Mapping in an Urban Environment from Hyperspectral and LiDAR-Derived Attributes. *Front. Plant Sci.* **2016**, *7*, 1528. [CrossRef] [PubMed]
85. Wang, L. Invasive Species Spread Mapping Using Multi-Resolution Remote Sensing Data. *Int. Arch. Photogramm. Remote Sens. Spat. Inf. Sci.* **2008**, *37*, 135–142.
86. Wang, C.; Liu, H.-Y.; Zhang, Y.; Li, Y.-F. Classification of land-cover types in muddy tidal flat wetlands using remote sensing data. *J. Appl. Remote Sens.* **2014**, *7*, 73457. [CrossRef]
87. Lu, D.; Hetrick, S.; Moran, E. Land Cover Classification in a Complex Urban-Rural Landscape with QuickBird Imagery. *Photogramm. Eng. Remote Sens.* **2010**, *76*, 1159–1168. [CrossRef] [PubMed]
88. Liu, M.; Li, H.; Li, L.; Man, W.; Jia, M.; Wang, Z.; Lu, C. Monitoring the Invasion of Spartina alterniflora Using Multi-source High-resolution Imagery in the Zhangjiang Estuary, China. *Remote Sens.* **2017**, *9*, 539. [CrossRef]
89. Suyadi; Gao, J.; Lundquist, C.J.; Schwendenmann, L. Land-based and climatic stressors of mangrove cover change in the Auckland Region, New Zealand. *Aquat. Conserv. Mar. Freshw. Ecosyst.* **2019**, *29*, 1466–1483. [CrossRef]

90. Udoidiong, O.M.; Ekwu, A.O. Nipa palm (*Nypa fruticans* wurmb) and the intertidal epibenthic macrofauna east of the imo river estuary, Nigeria. *World Appl. Sci. J.* **2011**, *14*, 1320–1330.
91. Twumasi, Y.A.; Merem, E.C. GIS and Remote Sensing Applications in the Assessment of Change within a Coastal Environment in the Niger Delta Region of Nigeria. *Int. J. Environ. Res. Public Health* **2006**, *3*, 98–106. [CrossRef] [PubMed]
92. Ayanlade, A. *Remote Sensing of Environmental Change in the Niger Delta, Nigeria*; King's College London, University of London: London, UK, 2014.